Paleoceanographic inferences from benthic foraminifera across the early Aptian Ocean Anoxic Event 1a in the western Tethys

Victor M. Giraldo-Gómez[a*], Maria Rose Petrizzo[a], Elisabetta Erba[a], Cinzia Bottini[a]

[a]Università degli Studi di Milano, Dipartimento di Scienze della Terra "A. Desio", Via Mangiagalli 34, 20133 Milano, Italy.

[*]Corresponding author.

E-mail addresses: victor.giraldo@unimi.it (Victor M. Giraldo-Gómez), mrose.petrizzo@unimi.it (Maria Rose Petrizzo), elisabetta.erba@unimi.it (Elisabetta Erba), cinzia.bottini@unimi.it (Cinzia Bottini).

Keywords: OAE 1a; Cismon Core; anoxia; planktonic foraminifera; calcareous nannofossils; paleoceanography.

Abstract

The paleoenvironmental impact of the early Aptian Ocean Anoxic Event 1a (OAE 1a, ca. 121 Ma) has been investigated in detail in the Cismon Core (Lombardy Basin, western Tethys) by using different geochemical and micropaleontological proxies. We provide the first high-resolution data of benthic foraminiferal assemblages through the upper Barremian - lower upper Aptian stratigraphic interval. Benthic foraminifera data are integrated with calcareous nannofossil and planktonic foraminifera records to create a comprehensive characterization of bottom and surface waters across

OAE 1a. Benthic foraminiferal communities are indicative of a marked change in bottom-waters around the "nannoconid decline" (latest Barremian) due to increased flux of organic matter to the seafloor and intermittent dysoxic conditions probably promoted by pulses of higher productivity during the initial Greater Ontong Java Event (GOJE). Benthic foraminifera experienced a marked crisis in abundance ("benthic foraminiferal crisis" BFC) ca. 35 kyr before the OAE 1a, in correspondence with the "nannoconid crisis" and the onset of the most intense GOJE phase. The literature survey shows that the BFC is commonly recorded before the OAE 1a onset in several stratigraphic sections worldwide, and therefore, it is here proposed as a global event. At Cismon, deep-water anoxia was reached at the OAE 1a onset and lasted for ca. 300 kyr, promoted by higher productivity and eventually enhanced water stratification during the super-greenhouse climate. The continuation of OAE 1a was marked by a benthic foraminiferal repopulation event, probably resulting from the influx of relatively cooler and oxygenated waters. In turn, the OAE 1a was marked by intermittent anoxic to dysoxic conditions, likely in response to primary productivity sustained by N-fixing bacteria. The distribution and abundance of benthic foraminifera documented in other sections across the Selli Level equivalent show different features that point to local factors such as paleodepth and increased runoff. The post-OAE 1a was characterized by dysoxic conditions coupled with moderate organic matter flux to the seafloor. At the Cismon site and worldwide, the termination of OAE 1a coincided with the return of relatively more abundant benthic taxa in response to the restoration of favorable conditions allowing the development of diversified benthic foraminiferal communities.

1. Introduction

The Cretaceous was punctuated by episodes of widespread deposition of organic-rich sediments (black shales) in the oceans and epicontinental seas, named Oceanic Anoxic Events (OAEs; Schlanger and Jenkyns, 1976), representing major alterations in the global carbon budget (Jenkyns, 2010). The

early Aptian OAE 1a (ca. 120.7 Ma, Malinverno et al., 2012) coincided with global paleoclimatic and paleoenvironmental perturbation that lasted for ca. 1.1 Myr (Malinverno et al., 2010) and probably triggered by volcanogenic CO_2 emissions associated with the Greater Ontong Java Event (GOJE, e.g., Larson, 1991; Erba, 1994; Bralower et al., 1994; Larson and Erba, 1999; Jones and Jenkyns, 2001; Leckie et al., 2002; Jenkyns, 2003; Méhay et al., 2009; Tejada et al., 2009; Bottini et al., 2012, 2015; Erba et al., 2015; Naafs et al., 2016; Percival et al., 2021). The release of methane hydrates has been proposed as an additional source of ^{12}C-enriched carbon (Beerling et al., 2002; van Breugel et al., 2007; Méhay et al., 2009; Malinverno et al., 2010; Adloff et al., 2019), which possibly further contributed to the negative carbon isotope anomaly at the OAE 1a onset (e.g., Weissert, 1989; Weissert and Lini, 1991; Jenkyns, 1995; Bralower et al., 1999; Erba et al., 1999, 2015; Luciani et al., 2001; Price, 2003; Ando et al., 2008; Méhay et al., 2009; Malkoç et al., 2010; Stein et al., 2011; Bottini et al., 2012, 2015; Lübke and Mutterlose, 2016; Frau et al., 2018). The positive excursion that follows the negative shift has been associated with an enhanced burial of organic carbon in marine sediments, either after increased surface-water productivity or preservation of organic matter (e.g., Arthur et al., 1987, 1988; Schlanger et al., 1987; Jenkyns, 2010; Robinson et al., 2017). These conditions led to the deposition of marine carbon-rich sediments (primarily black shales) known as the Selli Level in the Tethys (Coccioni et al., 1989), Niveau Goguel in France (Bréhéret, 1988) and Fischschiefer in the Lower Saxony Basin (Mutterlose and Böckel, 1998). To date, there is a comprehensive characterization of surface-water conditions during OAE 1a in the western Tethys (Premoli-Silva et al., 1999; Erba, 2004; Erba et al., 2019 and references therein), and there is a general understanding of bottom-water evolution across OAE 1a, including oxygenation and organic carbon flux (e.g., Kuypers et al., 2004; Pancost et al., 2004). In this regard, some indications are provided by benthic foraminifera, which are controlled by oxygen and food availability in bottom-waters (e.g., Sliter and Barker, 1972; Nyong and Olsson, 1984; van Morkhoven et al., 1986). In particular, studies on Tethyan sites (Cobianchi et al., 1999; Coccioni et

al., 2006; Michalík et al., 2008; Patruno et al., 2015; Józsa et al., 2016) and sections worldwide (Elkhazri et al., 2013; Bargen and Lehmann, 2014; Zorina et al., 2017) are suggestive of a decrease in benthic foraminifera abundance before OAE 1a. Several locations show scarce or absent benthic specimens during OAE 1a, possibly, in response to a major paleoenvironmental perturbation at the seafloor (Mutterlose and Böckel, 1998; Cobianchi et al., 1999; von Bargen and Lehmann, 2014). However, the relatively low sampling resolution adopted in these studies and/or the absence of a continuous benthic foraminiferal record through OAE 1a hamper a comprehensive characterization of the benthic foraminiferal response to OAE 1a. This is also verified in the Selli Level in the proposed stratotype in the Umbria-Marche Basin (Gorgo a Cerbara section, central Italy), which lacks benthic foraminifera (Patruno et al., 2015). Conversely, the Selli Level of the Cismon Core (Lombardy Basin, western Tethys, Italy) contains benthic foraminifera and, therefore, is ideal for your investigation through OAE 1a.

In this work, we performed a high-resolution investigation of the upper Barremian to lower upper Aptian stratigraphic interval of the Cismon Core, intending to (a) reconstruct the changes in the bottom-water oxygen conditions and organic carbon fluxes; (b) infer the paleobathymetry of the upper Barremian-lower upper Aptian sedimentary sequence of the Cismon Core; (c) assess the impact of the paleoceanographic perturbation associated with OAE 1a on the benthic foraminiferal communities; (d) integrate the benthic foraminiferal record with the calcareous nannofossil and planktonic foraminiferal datasets to produce a model of bottom- to surface-water changes across the OAE 1a in the Belluno Basin; and (e) compare the benthic foraminiferal assemblages of the Cismon Core with the records previously published from other localities to provide a comprehensive model of local vs. global paleoenvironmental perturbations across OAE 1a.

2. Geological setting and lithology

The Cismon Core was drilled in the Venetian Prealps (Southern Alps, NE Italy; Fig. 1), west of Feltre (Belluno Basin), along the Passo Rolle road at km 52.6 (46°02'43.46" N; 11°45'46.85" E; 398 m altitude). The studied interval covers 38.75 m and is represented by the Biancone Formation (upper Barremian to lowermost Aptian) and the Scaglia Variegata Formation (lower to upper Aptian). Lithostratigraphically, the Biancone Formation, a local equivalent of the Maiolica Limestone, consists of dominant limestones with intercalated black shales, and radiolarian-rich layers. The Scaglia Variegata Formation is characterized by marlstones, marly limestones, black shales and radiolarian beds (e.g., Erba and Larson, 1998; Erba et al., 1999).

The Selli Level equivalent corresponds to the OAE 1a in the Cismon Core and is found in the Scaglia Variegata Formation between 23.67 and 18.77 m (Fig. 2). The Selli Level is lithologically subdivided into three intervals: i) the lower interval (23.67 – 22.36 m) is constituted by marlstones with frequent black shales and a few discrete radiolarian beds; ii) a middle interval (22.36 – 20.41 m) consisting of limy marlstones with rare black shales and radiolarian beds; and iii) an upper interval (20.41 – 18.77 m) characterized by alternating marlstones, common radiolarian beds and black shales (Erba et al., 1999; Premoli-Silva et al., 1999). A negative $\delta^{13}C_{carb}$ shift (1 ‰) in the carbonate fraction characterizes the base of the Selli Level and is followed by a complex $\delta^{13}C_{carb}$ excursion (Menegatti et al., 1998; Erba et al., 1999; Bottini et al., 2015).

The sedimentary sequence was deposited on the Tethys southern margin (Fig. 1), on the eastward deepening slope between the Trento Plateau and the Belluno Basin, at an estimated paleo-depth of 1000–1500 m during the Early Cretaceous (Weissert and Lini, 1991; Erba and Larson, 1998; Bernoulli and Jenkyns, 2009; Erba et al., 2010).

3. Materials and methods

A total of 159 samples were studied for benthic foraminifera in the interval from 46.75 m to 8.00 m (Fig. 2), dated as the latest Barremian to early late Aptian (Erba et al., 1999). The benthic foraminiferal studied samples are the same as those investigated by Premoli Silva et al. (1999) and Barchetta (2015) for planktonic foraminifera. The sampling resolution varies from 5 to 50 cm in the interval from 8 m to 31.29 m and from 12 to 170 cm in the lower part (31.29 m – 46.75 m). The studied samples include different lithologies such as marly layers, radiolarian beds, marly limestones, and black shales. Following the results of Premoli Silva et al. (1999), the radiolarian beds often contain well preserved and relatively abundant planktonic and benthic foraminifera specimens, whereas the marly layers and black shales may have rare and poorly preserved specimens.

Originally, samples were prepared using two methods according to the lithology (Premoli Silva et al., 1999). Softer sediments were soaked in hydrogen peroxide for a few hours and then sieved through a 45-μm mesh-size to get foraminifera, while hard-siliceous samples were soaked in a 10% hydrochloric solution and sieved through a 63-μm mesh-size to extract radiolaria (Premoli Silva et al., 1999; Barchetta, 2015). The whole residues of the size-fraction > 63-μm were analyzed, and all benthic foraminifera were picked in each sample. Subsequently, all specimens were identified at genus and species level, counted, and stored in Plummer slides. Thin sections studied by Premoli Silva et al. (1999) and Barchetta (2015) were not investigated in this work because benthic foraminifera are too small to be confidently identified at species and genus level.

Absolute abundances of benthic foraminifera were calculated after weighing the washed residues, and the results are reported as Benthic Foraminiferal Number (BFN), corresponding to the number of individuals per gram of washed residue (n/g) in each sample. Species richness (S), Dominance (D), and Shannon diversity (H_S; Shannon and Weaver, 1949) were calculated for each sample using the PAST software (Hammer et al., 2001). A confidence interval (CI: 95%) based on the Clopper-Pearson method (e.g., Suchéras-Marx et al., 2019) was applied to the benthic foraminiferal assemblages using the PAST

144 software (Hammer et al., 2001). This method assesses the statistical reliability of the analyzed data to
145 give a credible interpretation when the populations are variable. If the relative abundance is low, the CI
146 is wider, whereas high relative abundance values display a narrower CI (Fig. 2).

147 Benthic foraminifera were identified at the species level when possible, following the taxonomy
148 by Ellis and Messina (1940-2015), Mjatliuk (1988), Weidich (1990), Meyn and Vespermann (1994),
149 Holbourn and Kaminski (1997), and Patruno et al. (2015). The most common taxa identified in the
150 Cismon Core were photographed using the Scanning Electron Microscopy (Jeol JSM-IT500) at the
151 Department of Earth Sciences of the Università degli Studi di Milano. Benthic foraminiferal taxa were
152 subdivided into two different morphogroups according to their life preferences: infauna and epifauna
153 (e.g., Koutsoukos, 1989; Murray and Alve 1999; Jorissen et al., 2007). A third group called epifauna–
154 infauna is here distinguished and includes opportunistic benthic foraminifera taxa adapted to variable
155 ecological niches and changing environmental conditions. We adopted the benthic foraminifera
156 paleobathymetric subdivision proposed by Nyong and Olsson (1984) and van Morkhoven et al. (1986)
157 as follows: inner-neritic (IN: 0 – 50 m), middle-neritic (MN: 50 – 100 m), outer-neritic (ON: 100 – 200
158 m), upper bathyal (UB: 200 – 500 m), middle bathyal (MB: 500 – 1000 m), and lower bathyal (LB:
159 1000 – 2000 m).

160 Planktonic foraminiferal absolute abundance data and species richness are here revised after
161 Premoli Silva et al. (1999) and Barchetta (2015). Absolute abundances in the washed residues (PFNwr)
162 were calculated as the number of individuals per gram of washed residue (n/g), whereas absolute
163 abundances in thin sections (PFNts) were obtained by counting the individuals in 40 fields of view
164 randomly chosen using a 125X magnification and corresponding to a total area of 80.4 mm^2.
165 Specimens analyzed in the washed residues are subdivided into morphogroups, according to the main
166 morphologies as follows: planispiral (genus *Globigerinelloides*, including species with globular and
167 radially elongate chambers; Verga and Premoli Silva, 2003a, 2003b, 2005), pseudo-planispiral (genus

Leupoldina characterized by possessing radially elongate chambers ending with close, bulb-shaped extensions; Verga and Premoli Silva, 2002) and trochospiral taxa (genera *Hedbergella*, *Lilliputianella*, *Gorbachikella* and *Gubkinella* characterized by having globular to radially elongate chambers; see Huber et al., 2016 and references therein).

4. Results

4.1 Benthic foraminiferal abundance and diversity

A total of 73 taxa (29 genera and 44 species) of benthic foraminifera were identified in the upper Barremian – upper Aptian interval of the Cismon Core (Supplementary Table S1). The BFN ranges from 1/g to 323/g, with an exception in sample 44.53 m that contains 1359/g (Fig. 2). Samples comprised between the base of the studied interval (46.75 m) and the base of the Selli Level (23.67 m) show an average BFN of 67/g. Within the Selli Level, the interval between 23.67 m and 21.89 m is barren of benthic foraminifera, while the overlaying interval of the Selli Level from 21.77 m to 18.83 m shows an average BFN of 3/g. The BFN above the Selli Level (18.43 to 8.20 m) is relatively low, with an average value of 12/g. The S fluctuates between 1 taxon in most samples and a maximum of 26 taxa in sample 15.98 m. The average S value in the studied section is 4 taxa (Fig. 2). The D ranges from 0.12 to 1 (Fig. 2): low values were mainly recorded in the upper Barremian (from 46.75 m to 32.30 m). Higher values are characteristic of the lower Aptian interval (below the Selli Level, from 27.19 m to 24.33 m), and the samples from above the barren interval, until the top of the studied stratigraphic section (from 21.77 m to 8.87 m). The H_S shows values from 0 to 2.2 (Fig. 2): most samples display low values, especially in the lower Aptian below the Selli Level (from 29.06 m to 23.66 m) and above the barren interval till the top of the studied stratigraphic section (from 21.77 m to 8.87 m).

Agglutinated foraminifera (AF) are recorded in 82% of the studied samples and constitute the most abundant group, varying from 1/g to 1365/g in abundance. Higher abundance values are detected

192 in the upper Barremian (from 46.75 m to 39.65 m), with a peak in sample 44.53 m containing 1365/g.
193 Lower abundances of AF are observed from 21.77 m to the top of the studied interval. The calcareous
194 benthic foraminifera (CF) are present in 66% of the samples, although with a limited abundance of 1/g
195 (in most samples) to 55/g in sample 21.46 m. The relative abundance of CF ranges from 0.6% (35.02
196 m) to 100% in most of the Selli Level samples (above the barren interval; Fig. 2).

197 The epifaunal morphogroup fluctuates from 1/g (16.44 m) to 704/g (44.53 m) and its relative
198 abundance varies from 3.9% (30.63 m) to 100% (in samples 27.34 m, 26.07 m, 25.65 m, 25.25 m,
199 24.64 m, 24.33 m, 11.02 m, 10.76 m). This morphogroup shows the highest abundances (up to 800/g)
200 from 46.75 m to 24.12 m. A decrease in abundance of the epifaunal morphogroup is recorded in sample
201 21.77 m, and the average abundance decreases toward the top of the studied interval. The exception is a
202 peak value of 123/g at 15.98 m (Fig. 2). The infaunal morphogroup ranges from 1/g (16.44 m) to 133/g
203 (26.59 m) and is more abundant in the upper Barremian and lowermost Aptian interval (mean value:
204 16/g). Above the Selli Level, the infaunal morphogroup displays very low abundances, reaching a
205 maximum value of 8/g (Fig. 2). The relative abundance of the infaunal morphogroup ranges from 1.2%
206 (15.98 m) to 100%, the latter abundance being observed in samples 28.85 m, 24.99 m, 20.53 m, 19.68
207 m, 19.01 m, 18.83 m, 9.72 m, and 9.31 m.

208 The opportunistic taxa included within the epifauna-infauna group fluctuate from 1/g (16.44 m)
209 to 583/g (44.53 m). An increase in abundance (up to 583/g) of this group is recorded in the upper
210 Barremian (44.53 m, 43.92 m, 43.41 m) and lower Aptian (15.98 m) interval. The relative abundance
211 of this group ranges from 3.1% (30.85 m) to 100% (in samples 20.47 m, 20.27 m, 19.53 m, 17.08 m,
212 18.86 m, 14.39 m; Fig. 2).

213 Six benthic foraminiferal intervals (BFI) were identified according to the variations in BFN, D,
214 and H_S (Fig. 2). From the base to the top, the BFIs are described as follows:

215 • BFI-I (46.75 m – 42.48 m) is characterized by moderate to high BFN and moderate H_S and D.

- BFI-II (42.48 m – 30.85 m) shows lower BFN, contains a few barren samples, and displays intermediate H_S and low D.
- BFI-III (30.85 m – 24.12 m) displays slightly higher BFN, intermediate H_S, and higher D.
- BFI-IV (24.12 – 21.77 m) is characterized by a marked decrease in BFN and H_S, but relatively high D just below the base of the Selli Level, while benthic foraminifera are absent in the Selli Level.
- BFI-V (21.77 m – 18.77 m) shows low BFN with intercalated barren samples, low H_S, and high D.
- BFI-VI (18.77 m – 8.20 m) shows intermediate BFN with few barren samples and is characterized by moderate H_S and intermediate to high D.

4.2 Composition of the benthic foraminiferal assemblages

Agglutinated and calcareous benthic foraminifera, recorded in the Cismon Core (Figs. 2, 3, and 4), were grouped according to their paleoecological affinities and abundances (Fig. 5 and Table 1).

4.2.1 Agglutinated benthic foraminifera (AF)

Two genera of agglutinated foraminifera are dominant in the Cismon Core (Fig. 5), *Rhizammina* and *Verneuilinoides*. The absolute abundance of *Rhizammina* ranges from 1/g (16.44 m) to 694/g (44.53 m). The highest abundances are recorded in the BFI-I (mean 85/g). The BFI-II shows lower abundance values of *Rhizammina*, although a minor increase is detected in the uppermost part of the interval. A few minor peaks are detected in the BFI-III, reaching 80/g (sample 32.30 m). The genus *Rhizammina* is absent in the Selli Level except for a few specimens found immediately above the barren interval. Low abundances of *Rhizammina* (mean value: 7/g) are recorded above the Selli Level (BFI-VI) except for a peak of 93/g observed at 15.98 m.

The genus *Verneuilinoides* is mainly represented by *Verneuilinoides* cf. *V. neocomiensis*, which displays an absolute abundance of 1/g (45.07 m) to 115/g (26.59 m). This species occurs only in the upper Barremian (BFI – I, II, and III). Peaks in abundance of *Verneuilinoides* cf. *V. neocomiensis* are recorded in a few samples from BFI-II (samples 36.66 m and 34.21 m) and BFI-III (samples 30.63 m, 29.42 m, 26.82 m, and 26.59 m).

Other agglutinated foraminifera displaying intermediate to low absolute abundances are documented in the Cismon Core. The genus *Ammodiscus* (*A. cretaceous*, *A. infimus*) is characterized by low absolute values varying from 1/g (18.78 m) to 6/g (15.18 m). Peaks in abundance of *Ammodiscus* are reported: in BF-I, at the top of BFI-II, in the middle of BFI-III, and in BFI-VI. The genus *Bathysiphon* (*B. brosgei*, *B. vitta*) ranged from 1/g (18.78 m) to 10/g (44.53 m) and was sporadically found throughout all the BFIs. This genus reaches the highest abundance in BFI-I (44.53 m). The genus *Dorothia* ranges from 1/g (25.09 m) to 16/g (26.59 m). The most significant increases in abundance of *Dorothia* are observed in one sample of BFI-I (43.41 m) displaying 14/g and in BFI-III (26.82 m and 26.59 m) with 10/g and 16/g, respectively.

Glomospira charoides and *Glomospira gordialis* are recorded in the BFI-I, BFI-II, and BFI-VI. *Glomospira charoides* displays low absolute abundances ranging from 2/g (BFI-I: 39.86 m) to 12/g (BFI-V: 15.98 m) and is the rarest taxon of the assemblages. On the contrary, *G. gordialis* displays more fluctuations in the absolute abundance with values comprised between 1/g (29.95 m) and 229/g (44.53 m). The maximum increases in abundance of *G. gordialis* are recorded in the BFI-I and BFI-II, but their peak in abundance is observed at 15.98 m (BFI-VI).

The genus *Haplophragmoides* (*H. kirki*, *H. gigas gigas*, *H. gigas minor*) was recorded in the BFI-I, BFI-II, BFI-III, and BFI-VI, varying in abundance values from 1/g (45.07 m, 35.02 m) to 120/g (43.41 m), and displaying peaks mainly in the BFI-I (46.75 m – 42.48 m). *Hippocrepina depressa*

shows low abundances ranging from 1/g (15.11 m) to 6/g (27.34 m) in the BFI-II, BFI-III, and BFI-VI. The highest abundance (6 /g; 27.34 m) of this species was recorded in the BFI-III.

The genus *Reophax* (*R. helveticus, R. liasicus*) displays low absolute abundances of 1/g (21.77 m) to 78/g (44.53 m). It is distributed through all BFIs, being more abundant in the BFI-I (44.53 m). The absolute abundance of Textularids shows values from 1/g (26.59 m) to 248/g (44.53 m) in the BFI-I, BFI-II, and BFI-III and registers the highest values in the BFI-I (44.53 m).

Other agglutinated taxa include *Ammobaculites* sp., *Binominela entis, Gaudryina dividens, Scherochorella minuta*, *Spiroplectinata lata*, *Tolypammina* sp., and *Tritaxia pyramidata,* all characterized by low absolute abundances (Supplementary Table S1).

4.2.2 Calcareous benthic foraminifera (CF)

The genus *Astacolus* (*A. calliopsis*, *A. humilis*, *A. planiusculus*) was recorded in the BFI-I, BFI-III, BFI-V and BFI-VI intervals, with low absolute abundance values ranging from 1/g (17.78 m) to 6/g (15.98 m). This genus is recorded in the BFI-V, and BFI-VI (21.77 m – 8.20 m) within and above the Selli Level, with the highest abundance (6/g) observed at 15.98 m (Fig. 5).

Gavelinella barremiana displays intermediate absolute abundance, varying from 1/g (35.02 m) to 45/g (26.82 m) across all BFIs. Increases in the abundance of *G. barremiana* were observed in the BFI-III. Conversely, *Gavelinella intermedia* was detected in the BFI-V and is characterized by low absolute abundance values ranging from 1/g (18.90 m) to 12/g (15.98 m). *Gyroidina nítida* displays low abundances across the BFI-III, BFI-V and BFI-VI intervals and, particularly below and above the Selli Level, varying from 1/g (15.11 m) to 6/g (24.12 m).The genus *Lenticulina* (*L. macrodisca, L. muensteri, L. pulchella, L. subgaultina, L. turgidula*) was detected in all BFIs, showing intermediate abundance values from 1/g (45.07 m) to 47/g (21.46 m), with the highest abundance in the Selli Level (21.46 m).

The genus *Laevidentalina* (*L. distincta*, *L. linearis*, *L. soluta*) was exclusively observed in the BFI-III, BFI-V, and BFI-VI and displayed low absolute abundances ranging from 1/g (samples 21.23 m, 20.87 m, 19.01 m, 16.91 m) to 6/g (30.33 m).

Other calcareous taxa, such as *Dentalina comunis*, *Dentalina gracilis*, *Dentalina guttifera*, *Globulina Prisca*, *Guttulina* sp., *Gyroidina globosa*, *Lingulina* sp., *Lingulonodosaria nodosaria*, *Nodosaria* sp., *Pleurostomella reussi*, *Pyrulina* sp., *Saracenaria* spp., *Stilostomell*a sp., and *Vaginulinopsis* spp., are characterized by low absolute abundance (Supplementary Table S1).

5. Discussion

5.1 Paleobathymetry of the Cismon Core based on benthic foraminifera

Benthic foraminiferal habitats are defined by the abundance of genera and/or marker species that thrive at specific water depths. Cretaceous benthic foraminiferal assemblages are thought to indicate water depths, similar to modern ocean assemblage composition, and their association with mega- and microfauna, which are also linked to sedimentary features (Sliter and Barker, 1972).The taxa found in the Cismon Core are divided into four groups based on the maximum paleo-depth range reported in the literature (Table 2).

Group 1 includes taxa documented down to abyssal settings (3000 m), such as agglutinated foraminifera *Rhizammina* and *Verneuilinoides neocomiensis* that were adapted to upper bathyal to abyssal paleo-water depths (200 m – 3000 m). *Dorothia*, *Ammodiscus*, *Astacolus*, and *Bathisyphon* are inferred to have populated inner neritic to abyssal settings (0 – >3000 m), while *G. charoides* (50 – 3000 m) and *Gyroidina globosa* are documented from outer neritic to abyssal environments (100 – 3000 m).

Group 2 consists of taxa that lived in upper bathyal to lower bathyal environments (up to 2000 m), such as *Lenticulina*, *Haplophragmoides*, and *Reophax*, that are supposed to have thrived between 0

– 2000 m. The genus *Gavelinella* and *G. gordialis* are interpreted to have thrived in outer neritic to lower bathyal (50 – 2000 m) environments.

Group 3 includes taxa that live in lower bathyal environments (1500 m), such as *Gavelinella intermedia* and *Gyroidina nitida.*

Group 4 includes taxa that live down to 1000 m, such as *Dentalina* (0 – 1000 m), *Laevidentalina*, and *Pleurostomella* (50 m – 1000 m).

The benthic foraminifera taxa of Group 2 and Group 3 are the most abundant in the studied interval and indicate a lower bathyal paleo-water depth of about 1500 m. The presence of taxa belonging to Group 4 eventually constrains the paleo-depth at the Cismon site to 1000 m (Table 2), but due to the rarity of taxa belonging to Group 4, we conclude that the Cismon site was probably deposited at a paleo-depth of between 1000 and 1500 m (lower bathyal). This result is consistent with previous studies, which indicated a paleo-water depth of 1000 – 1500 m (e.g., Weissert and Lini, 1991; Erba and Larson, 1998; Erba et al., 1999).

Among the taxa identified in the Cismon Core, remarkable is the identification of *Gavelinella barremiana* in the assemblages, which suggests that this species was probably adapted to thrive in deeper water than previously reported (middle neritic to upper bathyal; e.g., Koutsoukos, 1989; Riegraf, 1989; Frenzel, 2000; Tyszka, 2006).

5.2 Bottom-water dynamics across OAE 1a

The Cismon Core is characterized by epifaunal and infaunal benthic foraminifera, indicating variations in bottom-water conditions (nutrient and oxygen availability) during the late Barremian-early late Aptian time interval according to the TROX model (Trophic conditions and oxygen concentrations; Jorissen et al., 1995; De Stigter, 1996; van der Zwaan et al., 1999; Jorissen et al., 2007). In particular, benthic foraminifera developed different test morphologies (planispiral,

trochospiral, biserial, etc.) that are used to identify morphogroups corresponding to specific microhabitats (e.g., Corliss, 1985; Corliss and Chen, 1988; Koutsoukos and Hart, 1990; Tyszka, 1994) (Table 1). The epifaunal morphogroup is composed of benthic foraminifera that thrived under well-oxygenated conditions such as *Rhizammina* and *Gavelinella*. *Rhizammina* is considered an indicator of low organic-flux (Koutsoukos, 1989; Koutsoukos and Hart, 1990; Tyska, 1994; Nagy et al., 1995; Kaminski and Kuhnt, 1995; van der Ekker et al., 2000; Rückheim et al., 2006; Patruno et al., 2015) and high oxygen conditions in different oligotrophic settings (Koutsoukos, 1989; Koutsoukos and Hart, 1990; Kaminski and Kuhnt, 1995; Szarek et al., 2000; Rückheim et al., 2006; Patruno et al., 2015). However, *Rhizammina* is also considered an opportunistic taxon as, in some records, there is evidence that it thrived under low oxygen content (e.g., Kaminski and Kuhnt, 1995; Cetean et al., 2008). *Gavelinella* also shows a wide range of habitats and has been interpreted to have thrived in oligotrophic-mesotrophic environments in both well and poorly oxygenated conditions (Koutsoukos, 1989; Koutsoukos and Hart, 1990; Friedrich and Erbacher, 2006; Friedrich and Hemleben, 2007).

Infaunal taxa are thought to tolerate oxygen-depleted conditions and, in some cases, high organic fluxes. The main component of the infaunal morphogroup is the agglutinated genus *Verneuilinoides* (e.g., Rückheim et al., 2006; Patruno et al., 2015), which was also recorded in well-oxygenated environments (Kuhnt, 1995; Szarek et al., 2000), and *Reophax* (Koutsoukos, 1989; Tyska, 1994; van Den Akker et al., 2000; Rückheim et al., 2006; Reolid et al., 2008; Cetean et al., 2011; Reolid and Ruiz, 2012). The genera *Laevidentalina* (Holbourn et al., 2001; Friedrich and Hemleben, 2007; Koch and Friedrich, 2012) and *Pleurostomella* are thought to have inhabited low oxygen water masses (Koutsoukos, 1989; Frenzel, 2000; Kaiho, 1994; Holbourn et al., 2001).

Some taxa of the epifaunal or shallow infaunal morphogroups are considered opportunistic due to tolerated high- to low-oxygen conditions (Jorissen et al., 2007). This opportunistic groups include the genera *Haplophragmoides*, *Glomospira* (Kuhnt and Kaminski, 1989; Koutsoukos and Hart, 1990;

Rückheim et al., 2006; Cetean et al., 2008; Reolid et al., 2008), and *Lenticulina* (Koutsoukos, 1989; Tyska, 1994; Kaiho, 1994; Frenzel, 2000; Holbourn et al., 2001; Reolid et al., 2008; Koch and Friedrich, 2012).

The dominance of the genus *Rhizammina* in the upper Barremian (BFI-I) indicates temporary oxic–dysoxic conditions at the seafloor under low to moderate organic carbon flux (Figs. 2, 5, 6). In the BFI-II, benthic foraminifera experienced a decrease in abundance, also indicated by the presence of several barren samples and a reduction in H_S and D values. The BFI-II is also coeval with the decline in abundance of *Rhizammina* and increased abundances of *Verneuilinoides* and *Glomospira* (Figs. 5, 6), suggesting interludes of lower oxygen levels (dysoxic conditions) and increased organic carbon flux at the water-sediment interface.

Benthic foraminiferal assemblages in the BFI-I and BFI-II were investigated only in centimetric marly beds; therefore, the interpretation of the bottom water conditions does not refer to the limestones of the Biancone Formation, which dominate the BFI-I and BFI-II. Thus, the marly beds are attributed to the episodic reduction of oxygen concentrations in bottom water during generally well-oxygenated conditions. The further decrease in benthic foraminiferal abundance values, diversity, and dominance is interpreted as intermittent dysoxic conditions and high organic flux at the seafloor during the BFI-III (Figs. 2, 6). In particular, we infer from the benthic foraminiferal assemblages of BFI-III that, in the latest Barremian-earliest Aptian, oxygenated conditions were interrupted by short-lived interludes of reduced oxygen levels in bottom waters and elevated organic matter flux. The low total organic carbon content (< 1 wt. %) in the BFI-II, and BFI-III, supports this interpretation. Isolated TOC peaks (e.g., 3.8 wt. % at 42.91 m and 1.8 wt. % at 41.56 m) coincide with darker, centimetric marlstone layers marked by impoverished benthic foraminiferal assemblages.

A pronounced decrease in benthic foraminiferal abundance, here named “benthic foraminiferal crisis” (BFC; near the base of the BFI-IV at 23.89 m, Figs. 6, 7), is recorded just before the OAE 1a

onset. From the BFC toward the base of the Selli Level, rare specimens belonging to *Bathysiphon*, *Gavelinella*, *Gyroidina nitida*, *Rhizammina*, and *Reophax* are found, suggesting a deterioration of bottom-water conditions coupled with the progressive decrease of the oxygen content (dysoxic–anoxic) and high organic carbon flux. Benthic foraminifera are absent from the base of the carbon isotopic segment Ap3 up to the lowermost part of segment Ap5 (Bottini et al., 2015; C3-C5 *sensu* Menegatti et al., 1998), possibly in response to anoxic bottom-water conditions, which promoted the organic matter preservation of the Selli Level black shales, as also testified by TOC enrichments (up to 6 wt%) (Figs. 6, 7). These episodes were probably intermittent, as evidenced by bioturbation patterns recorded by Menegatti et al. (1998).

At the base of the BFI-V, in correspondence with the beginning of isotopic segment Ap5 (Bottini et al., 2015; C5-C6 *sensu* Menegatti et al., 1998), benthic foraminifera document the onset of a repopulation event (*sensu* Friedrich, 2010). The presence of the genera *Astacolus*, *Lenticulina*, *Laevidentalina*, *Rhizammina* and *Reophax* indicates a moderate, but significant, re-oxygenation of the seafloor during OAE 1a, despite the persistence of intermittent anoxic to dysoxic conditions that favored the organic matter preservation in black shales enriched in TOC content (up to 8 wt %) (Figs. 6, 7).

The relatively higher benthic foraminiferal abundance, lower H_S, and high D detected above the Selli Level (Fig. 2; BFI-VI) are interpreted to reflect attenuated organic carbon flux and relatively oxygenated bottom-water conditions, although not fully oxygenated (Figs. 6, 7). The samples from BFI-VI mostly correspond to radiolarian layers and, consequently, are not representative of the whole Scaglia Variegata Formation and probably reflect interludes of relatively higher productivity and moderate organic flux (Premoli Silva et al., 1999).

5.3 Late Barremian – early late Aptian paleoenvironmental changes in the western Tethys

The benthic foraminifera data collected from the Cismon Core are used to trace the development of deep-water conditions in response to the paleoenvironmental perturbations associated with OAE 1a. The integration of benthic foraminifera with calcareous nannofossil and planktonic foraminifera data contributes to a comprehensive characterization of the paleoclimatic and paleoceanographic conditions of the late Barremian to the early-late Aptian time interval in the western Tethys.

5.3.1 The late Barremian – earliest Aptian time interval

The benthic foraminiferal assemblages of the BFI-I indicate that, in the late Barremian, the Cismon site was characterized by oxic–dysoxic conditions and low to moderate organic carbon flux at the seafloor. The change in benthic foraminiferal abundance and assemblage composition in the BFI-II indicate that temporary phases of moderate instability at the seafloor took place during the deposition of the upper Barremian pelagic limestones. In particular, there is evidence of short-lived interludes of relatively higher organic flux and dysoxia that led to the deposition of millimetric to centimetric dark grey-black marlstone layers (Figs. 2, 6).

A pronounced general impoverishment in the total benthic foraminiferal abundance occurred ca. 1 m.y. before the OAE 1a onset (BFI-III) and, remarkably, corresponds to the “nannoconid decline” at 31.50 m (NC, Figs. 2, 6, 7), a globally recognized biohorizon, which represents the onset of a nannoplankton crisis (Erba and Tremolada, 2004).

Several studies have found a link between the "nannoconid decline" and the onset of an early volcanic phase of the GOJE (Erba et al., 2015, and references therein), most likely as a result of combined surface-water acidification and pulses of higher surface-water fertility caused by injections of volcanogenic CO_2 and biolimiting trace metals (Larson, 1991; Erba, 1994; Larson and Erba, 1999;

Tejada et al., 2009; Méhay et al., 2009; Bottini et al., 2012, 2015; Erba et al., 2015; Charbonnier et al., 2016).

The benthic foraminifera data gathered in this study suggest that interludes of increased surface-water fertility probably also had a significant impact on the seafloor, promoting the organic matter flux and inducing temporary phases of expanded oxygen minimum zone with consequent impoverishment of the benthic foraminiferal population (BFI-III; Figs. 6, 8). It is not excluded that benthic foraminifera also directly suffered higher concentrations of toxic metals, as this happens in modern benthic foraminifera (e.g., Frontalini and Coccioni, 2012; Munsel et al., 2010; Munsel 2013). However, we underline that the Cismon site was distant from reconstructed hydrothermal sources (GOJE) and metal concentrations detected in the sediments are relatively low compared to GOJE-near sites (e.g., DSDP Site 463, see Erba et al., 2015).

The temporal matching of benthos and plankton responses detected in the upper Barremian of the Cismon Core is the first evidence that the GOJE-induced paleoenvironmental perturbation affected bottom- and surface-water biota concurrently (Figs. 6, 7, 8). This observation may suggest a supra-regional to global cause for the benthic foraminifera decline in abundance detected in the Cismon Core, which should be proved by examining other records worldwide.

So far, a correlatable change in the benthic foraminiferal assemblages and associated turnover has been documented only at Gorgo a Cerbara in the Umbria-Marche Basin (Italy) (Patruno et al., 2015), as time-interval equivalent sections studied elsewhere have been investigated at low sampling resolution (Fig. 9). At Gorgo a Cerbara and Cismon Core, benthic foraminifera assemblage composition and abundance show a marked increase in infaunal benthic species (e.g., *Verneulinoides*) during the latest Barremian, especially in the marly strata (Supplementary Figure 1). Specifically, at Gorgo a Cerbara, Patruno et al. (2015) identified a "*Verneuilinoides* acme*"* from the topmost part of the magnetochron M0 up to the "nannoconid crisis". The correspondence between the "*Verneuilinoides* acme*"* and the

nannofossil “pentaliths peak” was interpreted to reflect higher nutrient–recycling after increased freshwater input through runoff (Bellanca et al., 2002; Bersezio et al., 2002; Erba and Tremolada, 2004; Patruno et al., 2015). In the Cismon Core, abundant *Verneuilinoides* are detected in the middle part of the BFI-II and, similarly to Gorgo a Cerbara, in the BFI-III up to the “nannoconid crisis” (Fig. 2, and Supplementary material). Indeed, this interval corresponds to pulses of increased surface-water fertility (Bottini et al., 2015) and pentalith peaks (Erba and Tremolada, 2004). Moreover, the planktonic foraminiferal assemblages analyzed in the washed residues confirm meso-to eutrophic conditions in the surface waters based on the occurrence of abundant opportunistic trochospiral taxa, which cyclically alternate with rare leupoldinids and with a few planispirals, the latter inferred to be indicative of more mesotrophic regimes (Premoli Silva et al., 1999; Coccioni et al., 2006) (Figs. 6, 7).

5.3.2 The benthic foraminifera crisis and repopulation across OAE 1a

Benthic foraminifera display a marked decrease in the absolute abundance (BFC), just before the OAE 1a onset, and are absent from the base of the Selli Level up to the lowermost part of the carbon isotope segment Ap5 (BFI-IV; Figs. 6, 7). The onset of the BFC correlates with a GOJE volcanic pulse at the OAE 1a onset (e.g., Méhay et al., 2009; Kuroda et al., 2011; Bottini et al., 2012; Erba et al., 2015), responsible for a stepwise accumulation of volcanogenic CO_2 in the atmosphere, paralleled by nutrient enrichment, progressive warming (Bottini et al., 2015; Bottini and Erba, 2018), and trace metal spikes (e.g., V, Zn, and Cu; Erba et al., 2015; Figs. 6, 7, 8). Remarkably, the BFC occurred almost contemporaneously with the “nannoconid crisis” (NC), as the difference in the stratigraphic level (1 cm) is due to the different sampling resolutions used for nannofossil and benthic foraminiferal analyses. This correspondence, also identified at Gorgo a Cerbara (Patruno et al., 2015; Fig. 9, Supplementary Fig. 1), testsifies to the onset of highly fertile surface-water conditions, which favored higher photic zone coccoliths at the expense of nannoconids (Erba, 2004; Bottini et al., 2015; Bottini

476 and Erba, 2018) and initiated dysoxic/mesotrophic conditions under higher organic carbon flux to the
477 seafloor.

478 During this phase, from the BFC (23.89 m) and the "nannoconid crisis" (23.90 m) to just above
479 the base of the Selli level, planktonic foraminifera seem not to be affected and show an increase of 52/g
480 in the washed residues and 12 specimens/FOV in thin sections at 23.66 m and 23.57 m, respectively
481 (Fig. 6). Specifically, the integration of the data obtained from washed residues and thin sections
482 increases the resolution of the planktonic foraminiferal record and documents a peak in the absolute
483 abundance 10 cm above the base of the Selli level (23.67 cm). This value is immediately followed by
484 an interval characterized by a marked decrease in abundance of planktonic foraminifera coupled with a
485 change in the assemblage composition, which results in the assemblage being almost solely
486 characterized by leopoldinids (Fig. 6, 7), interpreted to be tolerant taxa. The delay in the response of
487 the planktonic foraminifera, compared to the benthic foraminifera and nannoconids, could be related to
488 the composition of lower Aptian planktonic assemblages. These are characterized by the lack of
489 oligotrophic and specialized taxa, being only composed of mesotrophic to eutrophic species (Coccioni
490 et al., 2006). The interval marked by scarce to absent planktonic foraminifera correlates with the core
491 of the interval barren of benthic foraminifera and coincides with the temporary absence of nannofossils
492 (Fig. 7; Erba et al., 2010). Quantitative and morphometric analyses of calcareous nannofossils
493 evidenced that the volcanogenic CO_2 emissions at the "nannoconid crisis" started a progressive
494 increase in surface-water acidification and a shallowing of the calcite lysocline (Erba et al., 2010).
495 After ~75 kyr from the beginning of the $\delta^{13}C$ negative shift (core of carbon isotope segment Ap3), the
496 calcite lysocline reached ~1200 m of paleowater depth with consequent severe dissolution at the
497 sediment/water interface and an absence of calcareous nannofossils, which lasted for ~70 kyr (Erba et
498 al., 2010; Figs. 6, 7, 8), during the most intense GOJE volcanism (Tejada et al., 2009; Bottini et al.,
499 2012; Charbonnier et al., 2016; Percival et al., 2021). Therefore, it may be plausible that ocean

acidification contributed to the abrupt decline in planktonic foraminiferal abundance recorded at 23.41 cm as well as to the temporary absence of benthic foraminifera (Figs. 6, 7, 8).

The new benthic foraminifera data at the Cismon site show that the OAE 1a paleoenvironmental perturbation, related to the GOJE volcanism, including not only maximum warming (e.g., Price 2003; Ando et al., 2008; Mutterlose et al., 2014; Bottini et al., 2015; Bottini and Erba, 2018), surface-water acidification (Wissler et al., 2003; Weisser and Erba, 2004; Erba et al., 2010), and trace-metal release (Erba et al., 2015), but also imposed deep-water anoxic "inhabitable" conditions for ca. 300 kyr in the earliest part of OAE 1a (adopting the time scale of Malinverno et al., 2010; Figs. 6, 7, 8). This is consistent with rapid oceanic deoxygenation evidenced by combined redox-sensitive geochemical proxies (Bauer et al., 2021). The GOJE activity probably induced chemical and physical changes in surface waters, stimulating primary productivity and consuming oxygen through organic matter oxidation, hence promoting dysoxic to anoxic conditions at the seafloor. Evidence of increased surface-water fertility is based on the calcareous nannoplankton Nutrient Index (NI: Bottini et al., 2015; Bottini and Erba, 2018) and is confirmed by the composition of planktonic foraminiferal assemblages that, as mentioned above, register the absence of the mesotrophic and specialized planispiral taxa (Coccioni et al., 2006) and the rarity of the more opportunistic trochospiral taxa (Premoli Silva et al., 1999), both balanced by the common occurrence of the eutrophic and low oxygen tolerant leupoldinids (Fig. 6 TOC spikes further suggest higher organic matter preservation in this interval (Fig. 6; Erba et al., 1999). We infer that the increased primary productivity generated a higher organic flux to the seafloor coupled with oxygen depletion after organic matter degradation. A contribution to surface-water fertility could have also come from hydrothermal trace metal enrichments (V, Zn, and Cu; Erba et al., 2015), riverine runoff as suggested by palynomorph assemblages (Hochuli et al., 1999), and accelerated weathering rates, as documented by the increase in siliciclastic sedimentation (Weissert, 1990) and by radiogenic osmium isotopic composition of seawater (Tejada et al., 2009; Bottini et al., 2012; Fig. 7, 8).

Consequently, bottom-water anoxia could have been promoted by enhanced water stratification following increased precipitation and continental runoff.

Benthic foraminifera indicate that after ca. 300 kyr of bottom-water anoxia, alternating anoxic to dysoxic conditions prevailed at the Cismon site until the end of OAE 1a (BFI-V; Figs. 6, 7) and favored the deposition of organic-rich sediments, as also testified by relatively high TOC content (up to 6 wt. %). The benthic foraminifera repopulation detected in the Cismon Core reflects the ability of several taxa (*Gavelinella*, *Gyroidina*, *Laevidentalina*, *Lenticulina*, *Pleurostomella, Reophax, Rhizammin*a) to adapt to ameliorated but still unstable conditions, with alternating phases of anoxia and dysoxia at the seafloor (Figs. 6, 7, 8). The repopulation event was preceded by a relative cooling coincident with the end of the carbon isotope segment Ap3, the establishment of an intermediate temperature and the end of surface-water acidification (Erba et al., 2010; Bottini et al., 2015; Jenkyns, 2018; Huck and Heimhofer, 2021; Fig. 7). These changes in climatic and paleoenvironmental conditions were possibly favored by temporary inputs of relatively colder and more oxygenated waters, thereby inducing the benthic foraminifera return. Interludes of higher productivity were probably sustained by N-fixing cyanobacteria rather than by nannoplankton during BFI-V (see Kuypers et al., 2004; Dumitrescu and Brassell, 2006; Bottini et al., 2015), explaining the low nannofossil NI and the low abundances of the leupoldinids (Fig. 6).

In the Cismon Core, the benthic foraminiferal repopulation event coincides with a still low abundance of planktonic foraminifera, although a slight increase in species richness is registered (Fig. 6). Alternated anoxic to dysoxic conditions at the seafloor in the BFI-V interval were paralleled by changes in nutrient levels in surface waters, as testified by the composition of the planktonic foraminiferal assemblages. Specifically, the opportunistic trochospiral taxa dominating the assemblages cyclically fluctuated in abundance, alternating either with the specialized planispirals or with the opportunistic and eutrophic leupoldinids. This reveals a complex paleoceanographic scenario

548 characterized by high variability in the surface-water stratification. The benthic foraminiferal
549 repopulation coincides with relatively high calcareous nannofossil average abundance, similar to pre-
550 OAE 1a values in the photic zone (Fig. 7). The nannofossil assemblages indicate low fertility under
551 alternating minor cooler and warmer phases (Bottini et al., 2015).

552 Benthic foraminiferal repopulation events were documented for other OAEs, such as OAE 1b and
553 OAE 2, in response to moderate influxes of oxygen to the seafloor, temporarily interrupting anoxic
554 conditions (Eicher and Worstell, 1970; Erbacher et al., 1999; Holbourn and Kuhnt, 2001; Holbourn et
555 al., 2001; Friedrich et al., 2005, 2006; Friedrich, 2010). However, it is not possible to exclude that
556 benthic foraminifera were adapted to thrive in anoxic settings. This has been documented in new
557 studies of modern benthic foraminifera, which show their metabolic capacity to respire nitrate under
558 anoxic conditions (Risgaard-Petersen et al., 2006; Piña-Ochoa et al., 2010), allowing survival in anoxic
559 waters for weeks to months through denitrification (LeKieffre et al., 2017). Benthic foraminifera from
560 the Peruvian oxygen minimum zone also display a metabolic preference for denitrification over O_2
561 respiration (Glock et al., 2019). In the geological record, there are some examples of benthic
562 foraminifera that could survive long-term anoxic to dysoxic bottom-water conditions in denitrified
563 environments (Schneider-Mor et al., 2012; Quan et al., 2013; Belanger and Garcia, 2014; Meilijson et
564 al., 2015, 2018). Indeed, the benthic foraminiferal repopulation is concomitant with a period of
565 denitrification documented in the Cismon Core (Kuypers et al., 2004). This suggests an increase in the
566 nitrate and/or oxygen concentration in bottom-waters, favoring the return of benthic foraminifera even
567 under almost anoxic conditions.

568

569 **5.3.3 The post-OAE 1a phase**

570 The BFI-VI above the Selli Level (Figs. 7, 8) is characterized by the re-establishment of
571 oxygenated conditions at the seafloor, as indicated by a slight increase in the abundance of benthic

foraminifera. Meanwhile, in surface-waters, planktonic foraminifera display a marked increase in abundance and nannofossils also increase in abundance with the return of the nannoconids, indicating cooler and more oligotrophic surface-water conditions (Bottini et al., 2015). Similarly, abundant specialized planispiral taxa (Coccioni et al., 2006), which dominated over the trochospiral taxa and the leupoldinids, suggest more stable conditions and meso-to oligotrophic waters (Figs. 6, 7, 8). Our updated dataset, thus, advocates for a post-OAE 1a phase of coeval nannoplankton, planktonic foraminifera, and benthic foraminifera recovery under colder oligo-mesotrophic surface waters and more oxygenated conditions at the seafloor. The end of the GOJE volcanism and the burial of organic matter during OAE 1a — progressively acting as storage for excess CO_2 — most probably concurred to terminate OAE 1a and promote lower temperatures (Heimhofer et al., 2004; Bottini et al., 2015; Erba et al., 2015).

5.4 The worldwide benthic foraminiferal record across OAE 1a

The comparison of the benthic foraminiferal data of the Cismon Core with benthic foraminiferal records across OAE 1a from different localities (Coccioni et al., 1992; Mutterlose and Böckel 1998; Cobianchi et al., 1999; Rückheim et al., 2006; Michalík et al., 2008; Bargen and Lehmann 2014; Patruno et al., 2015; Moullade et al., 2015; Zorina et al., 2017) shows similarities and differences as discussed below (Fig. 9).

Several sites show a marked decrease in abundance (or disappearance) of benthic foraminifera before the OAE 1a onset (Coccioni et al., 1992; Mutterlose and Böckel 1998; Cobianchi et al., 1999; Rückheim et al., 2006; Bargen and Lehmann 2014; Patruno et al., 2015; Moullade et al., 2015; Zorina et al., 2017; Michalík et al., 2008), which correlates with the marked decrease in abundance (BFC) identified in the Cismon Core (Fig. 9). We infer that the BFC was a global event that may have occurred in response to the paleoenvironmental perturbation initiated just before the OAE 1a.

Contrarily, during OAE 1a, the benthic foraminifera abundance and composition were diverse in the studied localities (Fig. 9). The Cismon Core is the only section that displays an interval barren of benthic foraminifera in the early phase of OAE 1a, followed by a repopulation event occurring in the middle of OAE 1a. The Selli Level equivalent of some stratigraphic sections is entirely barren of benthic foraminifera (e.g., Coccioni et al., 1992; Michalík et al., 2008; Patruno et al., 2015; Zorina et al., 2017), whereas other sites are characterized by scarce specimens (Gargano: Cobianchi et al., 1999; Lower Saxony Basin, German: Mutterlose and Böckel 1998; Bargen and Lehmann 2014). Conversely, the Jebel Ammar section (Tunisia: Elkhazri et al., 2013) contains relatively common benthic foraminifera specimens, although the section only starts above segment Ap4 (Elkhazri et al., 2013). In the Lower Saxony Basin, higher benthic foraminifera abundances are reported at the end of the carbon isotope segment C6, close to the termination of OAE 1a (Mutterlose and Böckel 1998; Rückeim et al., 2006; Bargen and Lehmann 2014). The La Bedoule section in the Vocontian Basin (France) is the only site characterized by relatively frequent benthic foraminifera throughout the Niveau Goguel (Moullade et al., 2015), probably because anoxic conditions were never reached at this locality (Moullade et al., 2015).

Based on the high variability in the distribution of benthic foraminifera, we conclude that, during OAE 1a, the benthic community was primarily controlled by local factors. Remarkably, the benthic foraminifera record across the Selli Level in the Cismon Core also differs from other sections located in the western Tethys basins, such as the Umbria–Marche Basin (Gorgo a Cerbara section, central Italy: Coccioni et al., 1992; Patruno et al., 2015) and the Gargano Promontory (southern Italy: Cobianchi et al., 1999), further indicating that local environmental factors, possibly influenced by global paleoenvironmental changes related to OAE 1a, control the bottom-water oxygenation during OAE 1a.

The post-OAE 1a phase was instead marked by a typical response of the benthic foraminifera communities. Many stratigraphic sections display a recovery in benthic foraminiferal abundances

around the base of the carbon isotopic segment Ap7 indicative of restored oxygenated conditions at the seafloor after the termination of the OAE 1a (Coccioni et al., 1992; Mutterlose and Böckel 1998; Cobianchi et al., 1999; Elkhazri et al., 2013; Rückheim et al., 2006; Michalík et al., 2008; Józsa et al., 2016; von Bargen and Lehmann 2014; Patruno et al., 2015; Zorina et al., 2017; Fig. 9).

6. Conclusions

The study of the benthic foraminiferal assemblages in the Cismon Core provides, for the first time, a high-resolution record of bottom-water paleoceanographic conditions across the late Barremian to the early late Aptian time interval. The composition and abundance of the benthic foraminiferal assemblages confirm a paleowater depth for the Cismon Core of ca. 1000-1500 m (lower bathyal). The late Barremian was characterized by oxygenated conditions interrupted by short interludes of bottom-water dysoxia and high organic flux to the seafloor. In surface waters, the increase in fertilization caused a progressive decrease of the oligotrophic nannoconids ("nannoconid decline") and induced alternated phases of decrease and increase in abundance of the more specialized planispiral planktonic foraminiferal taxa. Before OAE 1a (ca. 35 kyr), benthic foraminifera were affected by a marked decrease in abundance, here named "benthic foraminifera crisis," coincident with the "nannoconid crisis" and contemporaneous with the initiation of the most intense GOJE volcanic phase. A profound change in the paleoenvironmental conditions occurred at the benthic and nannoconid crises level, including surface-water ocean acidification, progressive warming, increased surface-water fertility, and established deep-water dysoxia.

Bottom-water anoxia was reached at the OAE 1a onset, probably promoted by higher productivity under a super-greenhouse climate. Increased precipitation and continental runoff as a result of an accelerated hydrological cycle may also have contributed to an oxygen deficiency at the seafloor via enhanced water stratification.The anoxia caused the temporary absence of benthic foraminifera for ca.

300 kyr. Increased surface-water fertility also affected calcareous nannofossils and planktonic foraminifera assemblage composition but not their abundance. A benthic foraminifera repopulation event occurred after ca. 300 kyr from the OAE 1a onset, probably favored by the influx of relatively cooler and oxygenated waters. Intermittent anoxic to dysoxic conditions at the seafloor characterized the continuation of OAE 1a. Possibly, the interludes of higher productivity were sustained by N-fixing bacteria rather than by calcareous nannoplankton, indicating lower surface-water fertility. Accordingly, surface-water planktonic foraminifera show a change in the composition of their assemblages with the dominance of the opportunistic trochospiral taxa. The post-OAE 1a interval was characterized by the return of relatively abundant benthic foraminifera on a global scale, in response to the restoration of favorable conditions for the development of diversified communities of benthic foraminifera.

Acknowledgments

This research was funded through PRIN 2017RX9XXY to E. Erba. The authors acknowledge the support of the Italian Ministry of Education (MIUR) through the project “Dipartimenti di Eccellenza 2018–2022, Le Geoscienze per la Società: Risorse e loro evoluzione”. We thank the editor and anonymous reviewers for their helpful comments and suggestions. Thanks to Stefania Crespi for her assistance at the Scanning Electron Microscope.

CRediT authorship contribution statement

Victor M. Giraldo-Gómez: Conceptualization, Investigation, Data curation, Formal analysis, Visualization, Writing- original draft preparation, Writing - review & editing. **Maria Rose Petrizzo**: Supervision, Writing- Reviewing and Editing. **Elisabetta Erba**: Supervision, Writing- Reviewing and Editing, Funding acquisition. **Cinzia Bottini***:*Conceptualization, Writing- Original draft preparation, Writing - review & editing, Supervision.

References

Adloff, M., Greene, S. E., Parkinson, I. J., Naafs, B. D. A., Preston, W., Ridgwell, A., Monteiro, F. M., 2020. Unravelling the sources of carbon emissions at the onset of Oceanic Anoxic Event (OAE) 1a. Earth Planet. Sci. Lett. 530, 1-9. https://doi.org/10.1016/j.epsl.2019.115947.

Alegret, L., Molina, E., Thomas, E., 2003. Benthic foraminiferal turnover across the Cretaceous/Paleogene boundary at Agost (southeastern Spain): paleoenvironmental inferences. Mar. Micropaleontol. 48(3-4), 251-279.

Ando, A., Kaiho, K., Kawahata, H., Kakegawa, T., 2008. Timing and magnitude of early Aptian extreme warming: Unraveling primary $\delta^{18}O$ variation in indurated pelagic carbonates at Deep Sea Drilling Project Site 463, central Pacific Ocean. Palaeogeogr. Palaeoclimatol. Palaeoecol. 260, 463-476.

Arthur, M. A., Schlanger, S. T., Jenkyns, H. C., 1987. The Cenomanian-Turonian Oceanic Anoxic Event, II. Palaeoceanographic controls on organic-matter production and preservation. Geol. Soc. Spec. Publ. 26(1), 401-420.

Arthur, M. A., W. E. Dean, L. M. Pratt., 1988. Geochemical and climatic effects of increased marine organic carbon burial at the Cenomanian/Turonian boundary. Nature. 335, 714-716.

Ashckenazi-Polivoda, S., Titelboim, D., Meilijson, A., Almogi-Labin, A., Abramovich, S., 2018. Bathymetric trend of Late Cretaceous southern Tethys upwelling regime based on benthic foraminifera. Cretaceous Res. 82, 40-55.

Barchetta, A., 2015. The Tethys (Cismon core) and Pacific (DSDP Site 463) Ocean record of OAE1a: a taxonomic and quantitative analyses of planktonic foraminifera and their biological response across the Selli Level equivalent. Doctoral Thesis. Università degli Studi di Milano. Milano, Italy. 228 pp. (https://air.unimi.it/handle/2434/260289).

699 Beerling, D. J., Lomas, M. R., Gröcke, D. R., 2002. On the nature of methane gas-hydrate dissociation
700 during the Toarcian and Aptian Oceanic Anoxic Events. Am. J. Sci. 302, 28-49.
701
702 Belanger, C. L., Garcia, M. V., 2014. Differential drivers of benthic foraminiferal and molluscan
703 community composition from a multivariate record of early Miocene environmental change.
704 Paleobiology. 40(3), 398-416.
705
706 Bellanca, A., Erba, E., Neri, R., Silva, I. P., Sprovieri, M., Tremolada, F., Verga, D., 2002.
707 Palaeoceanographic significance of the Tethyan 'Livello Selli' (Early Aptian) from the Hybla
708 Formation, northwestern Sicily: biostratigraphy and high-resolution chemostratigraphic records.
709 Palaeogeogr. Palaeoclimatol. Palaeoecol.185(1-2), 175-196.
710
711 Bernoulli, D., Jenkyns, H. C., 2009. Ancient oceans and continental margins of the Alpine
712 Mediterranean Tethys: Deciphering clues from Mesozoic pelagic sediments and ophiolites.
713 Sedimentology. 56(1), 149-190.
714
715 Bersezio, R., Erba, E., Gorza, M., Riva, A., 2002. Berriasian–Aptian black shales of the Maiolica
716 formation (Lombardian Basin, Southern Alps, Northern Italy): local to global events. Palaeogeogr.
717 Palaeoclimatol. Palaeoecol. 180(4), 253-275.
718
719 Bindiu, R., Filipescu, S., Bălc, R., 2013. Biostratigraphy and paleoenvironment of the Upper
720 Cretaceous deposits in the northern Tarcău Nappe (Eastern Carpathians) based on foraminifera and
721 calcareous nannoplankton. Geol Carpath. 64(2), 117-132.
722
723 Blakey, R., 2012. Global paleogeography maps, library of paleogeography. Colorado Plateau
724 Geosystems Inc., Arizona, USA. http://cpgeosystems.com/paleomaps. html.
725
726 Bock, W. D., 1979. Upper Aptian agglutinated foraminifers from DSDP Hole 402A. Init. Rep. Deep
727 Sea Drill. Proj.48, 371-375.
728
729 Bottini, C., Erba, E., 2018. Mid-Cretaceous paleoenvironmental changes in the western Tethys. Clim.

Past. 14(8), 1147-1163.

Bottini, C., Cohen, A.S., Erba, E., Jenkyns, H. C., Coe, A. L., 2012. Osmium isotope evidence for volcanism, weathering and ocean mixing during the early Aptian OAE 1a. Geology. 40, 583-586.

Bottini, C., Erba, E., Tiraboschi, D., Jenkyns, H. C., Schouten, S., Sinninghe Damsté, J. S., 2015. Climate variability and ocean fertility during the Aptian Stage. Clim. Past. 11, (3), 383-402.

Bralower, T. J., Arthur, M. A., Leckie, R. M., Sliter, W. V., Allard, D. J., Schlanger, S.O., 1994. Timing and paleoceanography of oceanic dysoxia/anoxia in the late Barremian to early Aptian. Palaios. 9, 335-369.

Bralower, T. J., Cobabe, E., Clement, B., Sliter, W. V., Osburne, C., Longoria, J., 1999. The record of global change in mid-Cretaceous, Barremian-Albian sections from the Sierra Madre, northeastern Mexico. J. Foraminiferal Res. 29, 418-437.

Bréhéret, J. G., 1997. L'Aptien et l'Albien de la Fosse vocontienne (des bordures au bassin): Evolution de la sédimentation et enseignements sur les événements anoxiques. Bull. Soc. géol. Fr. 8, 1-614.

Bauer, K. W., Bottini, C., Frei, R., Asael, D., Planavsky, N. J., Francois, R., Crowe, S. A., 2021. Pulsed volcanism and rapid oceanic deoxygenation during Oceanic Anoxic Event 1a. Geology. 49, 1452-1456.

Cetean, C., Balc, R., Kaminski, M. A., Filipescu, S., 2008. Biostratigraphy of the Cenomanian-Turonian boundary in the Eastern Carpathians (Dâmboviţa Valley): preliminary observations. Studia UBB Geologia. 53(1), 11-23.

Cetean, C. G., Bălc, R., Kaminski, M. A., Filipescu, S., 2011. Integrated biostratigraphy and palaeoenvironments of an upper Santonian–upper Campanian succession from the southern part of the Eastern Carpathians, Romania. Cretaceous Res. 32 (5), 575-590.

761 Channell, J. E. T., Erba, E., Muttoni, G., Tremolada, F., 2000. Early Cretaceous magnetic stratigraphy in
762 the APTICORE drill core and adjacent outcrop at Cismon (Southern Alps, Italy), and correlation to
763 the proposed Barremian-Aptian boundary stratotype. Geol. Soc. Am. Bull. 112(9), 1430-1443.
764
765 Charbonnier, G., Morales, C., Duchamp-Alphonse, S., Westermann, S., Adatte, T., Föllmi, K. B.,
766 (2017). Mercury enrichment indicates volcanic triggering of Valanginian environmental change. Sci.
767 Rep. 7(1), 1-6.
768
769 Cobianchi, M., Luciani, V., Menegatti, A., (1999). The Selli Level of the Gargano Promontory, Apulia,
770 southern Italy: foraminiferal and calcareous nannofossil data. Cretaceous Res. 20(3), 255-269.
771
772 Coccioni, R., 1989. Stratigraphy and mineralogy of the Selli Level (Early Aptian) at the base of the
773 Marne a Fucoidi in the Umbrian-Marchean Apennines (Italy). In Cretaceous of the Western Tethys.
774 3rd International Cretaceous Symposium. Schweizerbart. pp. 563-584.
775
776 Coccioni, R., Erba, E., Premoli-Silva, I., 1992. Barremian-Aptian calcareous plankton biostratigraphy
777 from the Gorgo Cerbara section (Marche, central Italy) and implications for plankton evolution.
778 Cretaceous Res. 13(5-6), 517-537.
779
780 Coccioni, R., Luciani, V., Marsili, A., 2006. Cretaceous oceanic anoxic events and radially elongated
781 chambered planktonic foraminifera: paleoecological and paleoceanographic implications.
782 Palaeogeogr. Palaeoclimatol. Palaeoecol. 235 (1-3), 66-92.
783
784 Corliss, B. H., 1985. Microhabitats of benthic foraminifera within deep-sea sediments. Nature. 314
785 (6010). 435-438.
786
787 Corliss, B. H., Chen, C., 1988. Morphotype patterns of Norwegian Sea deep-sea benthic foraminifera
788 and ecological implications. Geology. 16 (8), 716-719.
789
790 De Azevedo, R. L. M., Gomide, J., Viviers, M. C., 1987. Geo-história da Bacia de Campos, Brasil: do
791 Albiano ao Maastrichtiano. Rev. Bras. Geociênc. 17(2), 139-146.

De Stigter, H.C., 1996. Recent and fossil foraminifera in the Adriatic Sea: distribution patterns in relation to organic carbon flux and oxygen concentration at the seabed. Geologica Ultraiectina. 144, 254 pp.

Dumitrescu, M., Brassell, S. C., Schouten, S., Hopmans, E. C., Sinninghe Damsté, J. S., 2006. Instability in tropical Pacific seasurface temperatures during the early Aptian. Geology, 34, 833-866.

Eicher, D. L., Worstell, P., 1970. Cenomanian and Turonian foraminifera from the great plains, United States. Micropaleontology. 16(3), 269-324.

Elkhazri, A., Abdallah, H., Razgallah, S., Moullade, M., Kuhnt, W., 2013. Carbon-isotope and microfaunal stratigraphy bounding the Lower Aptian Oceanic Anoxic Event 1a in northeastern Tunisia. Cretaceous Res. 39, 133-148.

Ellis, B. E., Messina, A. R., 1940-2015. Catalogue of Foraminifera. Micropaleontology Press, American Museum of Natural History, New York. Catalogue online. http://www.micropress.org.

Erba, E., 1994. Nannofossils and superplumes: The early Aptian 'nannoconid crisis'. Paleoceanography. 9, 483-501.

Erba, E., 2004. Calcareous nannofossils and Mesozoic oceanic anoxic events. Mar. Micropaleontol. 52(1-4), 85-106.

Erba, E., Larson, R., 1998. The Cismon Apticore (Southern Alps, Italy): "Reference section" for the Lower Cretaceous at low latitudes. Riv Ital Paleontol S. 104, 181-192.

Erba, E., Tremolada, F., 2004, Nannofossil carbonate fluxes during the Early Cretaceous: phytoplankton response to nutrification episodes, atmospheric CO_2 and anoxia. Paleoceanography. 19, 1-18.

Erba, E., Channell, J. E. T., Claps, M., Jones, C., Larson, R. L., Opdyke, B., Premoli Silva, I., Riva, A., Salvini, G., Torricelli, S., 1999. Integrated stratigraphy of the Cismon Apticore (Southern Alps, Italy): A “reference section” for the Barremian-Aptian interval at low latitudes. J. Foraminiferal Res. 29, 371-391.

Erba, E., Bottini, C., Weissert, J. H., Keller, C.E., 2010. Calcareous nannoplankton response to surface-water acidifi cation around Oceanic Anoxic Event 1a. Science. 329, 428-432.

Erba, E., Duncan, R. A., Bottini, C., Tiraboschi, D., Weissert, H., Jenkyns, H. C., Malinverno, A., 2015. Environmental consequences of Ontong Java Plateau and Kerguelen Plateau volcanism. The origin, evolution, and environmental impact of oceanic large igneous provinces. Geol. Soc. Am. Spec. Pap. 511, 271-303.

Erba, E., Bottini, C., Faucher, G., Gambacorta, G., Visentin, S., 2019. The response of calcareous nannoplankton to Oceanic Anoxic Events: The Italian pelagic record. Soc. Paleontol. Ital. 58, 51-71.

Erbacher, J., Hemleben, C., Huber, B. T., Markey, M., 1999. Correlating environmental changes during early Albian oceanic anoxic event 1B using benthic foraminiferal paleoecology. Mar. Micropaleontol. 38(1), 7-28.

Frau, C., Bulot, L. G., Delanoy, G., Moreno-Bedmar, J. A., Masse, J. P., Tendil, A. J. B., Lanteaume, C., 2018. The Aptian GSSP candidate at Gorgo a Cerbara (Central Italy): an alternative interpretation of the bio-, litho-and chemostratigraphic markers. Newsl Stratigr. 51(3), 311-326.

Frenzel, P., 2000. Die benthischen Foraminiferen der Rügener Schreibkreide (Unter-Maastricht, NE-Deutschland). Neues Palaontol Abh. 3. 1-361.

Friedrich, O., 2010. Benthic foraminifera and their role to decipher paleoenvironment during mid-Cretaceous Oceanic Anoxic Events–the “anoxic benthic foraminifera” paradox. Rev. de Micropaleontol. 53(3), 175-192.

Friedrich, O., Erbacher, J., 2006. Benthic foraminiferal assemblages from Demerara Rise (ODP Leg 207, western tropical Atlantic): possible evidence for a progressive opening of the Equatorial Atlantic Gateway. Cretaceous Res. 27 (3), 377-397.

Friedrich, O., Hemleben, C., 2007. Early Maastrichtian benthic foraminiferal assemblages from the western North Atlantic (Blake Nose) and their relation to paleoenvironmental changes. Mar. Micropaleontol. 62(1), 31-44.

Friedrich, O., Nishi, H., Pross, J., Schmiedl, G., Hemleben, C., 2005. Millennial-to centennial-scale interruptions of the Oceanic Anoxic Event 1b (Early Albian, mid-Cretaceous) inferred from benthic foraminiferal repopulation events. Palaios, 20(1), 64-77.

Friedrich, O., Erbacher, J., Mutterlose, J., 2006. Paleoenvironmental changes across the Cenomanian/Turonian boundary event (oceanic anoxic event 2) as indicated by benthic foraminifera from the Demerara Rise (ODP Leg 207). Rev. de Micropaleontol. 49(3), 121-139.

Frontalini, F., Coccioni, R., 2012. The response of the benthic foraminiferal community to copper exposure: the mesocosm experience. J. Environ. Prot. Sci. 3, 342-352.

Glock, N., Roy, A. S., Romero, D., Wein, T., Weissenbach, J., Revsbech, N. P., Dagan, T., 2019. Metabolic preference of nitrate over oxygen as an electron acceptor in foraminifera from the Peruvian oxygen minimum zone. PNAS. 116(8), 2860-2865.

Haig, D. W., 2005. Foraminiferal evidence for inner neritic deposition of Lower Cretaceous (Upper Aptian) radiolarian-rich black shales on the Western Australian margin. J Micropalaeontol. 24(1), 55-75.

Hammer, O., Harper, D. A. T., Ryan, P. D., 2001. PAST: paleontological statistics software package for education and data analysis. Palaeontol Electronica. 4, 1-9.

Heimhofer, U., Hochuli, P. A., Herrle, J. O., Andersen, N., Weissert, H., 2004. Absence of major

vegetation and palaeoatmospheric pCO2 changes associated with oceanic anoxic event 1a (Early Aptian, SE France). Earth Planet. Sci. Lett. 223(3-4), 303-318.

Hochuli, P. A., Menegatti, A. P., Weissert, H., Riva, A., Erba, E., Premoli Silva, I., 1999, Episodes of high productivity and cooling in the early Aptian Alpine Tethys: Geology. 27, 657-660.

Holbourn, E. L., Kaminski, M. A., 1997. Lower Cretaceous deep-water benthic foraminifera of the Indian Ocean (a synthesis of DSDP and ODP material). Grzyb Found Spec Pub. 4, 172 pp.

Holbourn, A., Kuhnt, W., 2001. No extinctions during oceanic anoxic event 1b: The Aptian-Albian benthic foraminiferal record of ODP Leg 171. Geol. Soc. Spec. Publ. 183(1), 73-92.

Holbourn, A., Kuhnt, W., Soeding, E., 2001. Atlantic paleobathymetry, paleoproductivity and paleocirculation in the late Albian: the benthic foraminiferal record. Palaeogeogr. Palaeoclimatol. Palaeoecol. 170 (3-4), 171-196.

Holbourn, A., Henderson, A. S., MacLeod, N., 2013. Atlas of benthic foraminifera. John Wiley & Sons. West Sussex, UK. 654 pp.

Huber, B.T., Petrizzo, M.R., Young, J.R., Falzoni, F., Gilardoni, S.E., Bown, P.R., Wade, B.S. (2016). Pforams@ mikrotax. Micropaleontology. 62 (6), 429-438.

Huck, S., Heimhofer, U., 2021. Early Cretaceous sea surface temperature evolution in subtropical shallow seas. Sci. Rep. 11(1), 1-9.

Jenkyns, H. C., 1995, Carbon-isotope stratigraphy and paleoceanographic signifcance of the lower Cretaceous shallow-water carbonates of Resolution Guyot, Mid-Pacific Mountains, in Winterer, E.L., Sager, W. W., Firth, J. V., and Sinton, J. M., eds., Proceedings of the Ocean Drilling Program, Scientific Results, Volume 143: College Station, Texas, Ocean Drilling Program. 99-104.

Jenkyns, H. C., 2003, Evidence for rapid climate change in the Mesozoic–Palaeogene greenhouse

world. Philos. Trans. R. Soc. Series A. 361, 1885-1916.

Jenkyns, H. C., 2010. Geochemistry of oceanic anoxic events. Geochem Geophys. 11(3), 1-30.

Jenkyns, H. C., 2018. Transient cooling episodes during Cretaceous Oceanic Anoxic Events with special reference to OAE 1a (Early Aptian). Philos. Trans. Royal Soc. A. 376(2130), 1-26.

Jones, C. E., Jenkyns, H. C., 2001. Seawater strontium isotopes, oceanic anoxic events, and seafloor hydrothermal activity in the Jurassic and Cretaceous. Am. J. Sci. 301, 112-149.

Jorissen, F. J., Destigter, H. C., Widmark, J. G. V., 1995, A conceptual model explaining benthic foraminiferal microhabitats. Mar. Micropaleontol. 26, 3-15.

Jorissen, F. J., Fontanier, C., Thomas, E., 2007, Paleoceanographical proxies based on deep-sea benthic foraminiferal assemblage characteristics. Dev. Mar. Geol. 1, 263-325.

Józsa, Š., Boorová, D., Filo, I., 2016. Aptian planktonic foraminiferal biostratigraphy and smaller benthic foraminifera from the Párnica Formation (Choč Mts., Western Carpathians). Acta Geol Slovaca. 8(1), 15-26.

Józsa, Š., 2017. Deep water agglutinated foraminifera from the Jurassic/Cretaceous boundary and paleoenvironmental settings of the Maiolica type facies from the Czorstyn ridge (Pieniny Klippen belt, western Carpathians). Riv Ital Paleontol S. 123(3), 395-405.

Kaiho, K., 1994. Benthic foraminiferal dissolved-oxygen index and dissolved-oxygen levels in the modern ocean. Geology. 22 (8), 719-722.

Kaminski, M. A., Kuhnt, W., 1995. Tubular agglutinated foraminifera as indicators of organic carbon flux. Grzyb Found Spec Pub. 3, 141-144.

Kaminski, M. A., Kuhnt, W., Moullade, M., 1999. The evolution and paleobiogeography of abyssal

947 agglutinated foraminifera since the Early Cretaceous: A tale of four faunas. Neues Jahrb Geol
948 Palaontol Abh. 212(1-3), 401-439.
949
950 Kaminski, M. A., Gradstein, F. M., 2005. Atlas of Paleogene cosmopolitan deep-water agglutinated
951 foraminifera. Grzyb Found Spec Pub. 10, 1-547.
952
953 Koch, M. C., Friedrich, O., 2012. Campanian-Maastrichtian intermediate-to deep-water changes in the
954 high latitudes: Benthic foraminiferal evidence. Paleoceanography. 27(2), 1-11.
955
956 Koutsoukos, E. A. M., 1989. Mid-to Late Cretaceous microbiostratigraphy, palaeo-ecology and
957 palaeogeography of the Sergipe Basin, northeastern Brazil. Ph.D. Thesis. University of Plymouth.
958 Plymouth, UK. 471 pp.
959
960 Koutsoukos, E. A. M., Hart, M. B., 1990. Cretaceous foraminiferal morphogroup distribution patterns,
961 palaeocommunities and trophic structures: a case study from the Sergipe Basin, Brazil. Earth Env
962 Sci t R So. 81 (03), 221-246.
963
964 Kuhnt, W., 1995. Deep-water agglutinated foraminifera from the Lower Cretaceous (Neocomian)
965 'Complex à Aptychus' Formation (Corridor de Boyar, Betic Cordillera, southern Spain). J
966 Micropalaeontol. 14(1), 37-52.
967
968 Kuhnt, W., Kaminski, M. A., 1989. Upper Cretaceous deep-water agglutinated benthic foraminiferal
969 assemblages from the Western Mediterranean and adjacent areas. In Cretaceous of the Western
970 Tethys. Proceedings of 3rd International Cretaceous Symposium. Schweizerbart. 91-120.
971
972 Kuroda, J., Tanimizu, M., Hori, R. S., Suzuki, K., Ogawa, N. O., Tejada, M. L., Ohkouchi, N., 2011.
973 Lead isotopic record of Barremian–Aptian marine sediments: Implications for large igneous
974 provinces and the Aptian climatic crisis. Earth Planet. Sci. Lett. 307(1-2), 126-134.
975
976 Kuypers, M. M. M., van Breugel, Y., Schouten, S., Erba, E., Sinninghe Damsté, J. S., 2004. N_2-fixing
977 cyanobacteria supplied nutrient N for Cretaceous oceanic anoxic events. Geology. 32, 853-856.

Larson, R. L., 1991. Geological consequences of superplumes. Geology. 19, 963-966

Larson, R. L., Erba, E., 1999, Onset of the mid-Cretaceous greenhouse in the Barremian–Aptian: Igneous events and the biological, sedimentary and geochemical responses. Paleoceanography. 14, 663-678.

Leckie, R. M., Bralower, T. J., Cashman, R., 2002. Oceanic anoxic events and plankton evolution: Biotic response to tectonic forcing during the mid-Cretaceous. Paleoceanography. 17(3), 13-1.

LeKieffre, C., Spangenberg, J. E., Mabilleau, G., Escrig, S., Meibom, A., Geslin, E., 2017. Surviving anoxia in marine sediments: The metabolic response of ubiquitous benthic foraminifera (Ammonia tepida). PloS One, 12(5), 1-21.

Li, Y. X., Bralower, T. J., Montañez, I. P., Osleger, D. A., Arthur, M. A., Bice, D. M., Silva, I. P., 2008. Toward an orbital chronology for the early Aptian oceanic anoxic event (OAE1a, ~ 120 Ma). Earth Planet. Sci. Lett. 271(1-4), 88-100.

Lübke, N., Mutterlose, J., 2016. The impact of OAE 1a on marine biota deciphered by size variations of coccoliths. Cretaceous Res. 61, 169-179.

Luciani, V., Cobianchi, M., Jenkyns, H. C., 2001, Biotic and geochemical response to anoxic events: The Aptian pelagic succession of the Gargano Promontory (southern Italy). Geol. Mag. 138, 277-298.

Malinverno, A., Erba, E., Herbert, T. D., 2010. Orbital tuning as an inverse problem: Chronology of the early Aptian oceanic anoxic event 1a (Selli Level) in the Cismon APTICORE. Paleoceanography. 25, 1-16.

Malinverno, A., Hildebrandt, J., Tominaga, M., Channell, J. E., 2012). M sequence geomagnetic polarity time scale (MHTC12) that steadies global spreading rates and incorporates astrochronology

constraints. J. Geophys. Res. Solid Earth. 117pp.

Malkoč, M., Mutterlose, J., Pauly, S., 2010. Timing of the early Aptian $\delta^{13}C$ excursion in the Boreal Realm. Newsl Stratigr. 43, 251-273.

Méhay, S., Keller, C. E., Bernasconi, S. M., Weissert, H., Erba, E., Bottini, C., Hochuli, P. A., 2009. A volcanic CO_2 pulse triggered the Cretaceous Oceanic Anoxic Event 1a and a biocalcification crisis. Geology. 37, 819-822.

Meilijson, A., Ashckenazi-Polivoda, S., Illner, P., Alsenz, H., Speijer, R. P., Almogi-Labin, A., Abramovich, S., 2015. Evidence for specific adaptations of fossil benthic foraminifera to anoxic–dysoxic environments. Paleobiology. 42(1), 77-97.

Meilijson, A., Ashckenazi-Polivoda, S., Illner, P., Speijer, R. P., Almogi-Labin, A., Feinstein, S., Abramovich, S., 2018. From phytoplankton to oil shale reservoirs: A 19-million-year record of the Late Cretaceous Tethyan upwelling regime in the Levant Basin. Mar. Pet. Geol. 95, 188-205.

Menegatti, A. P., Weissert, H., Brown, R. S., Tyson, R. V., Farrimond, P., Strasser, A., Caron, M., 1998. High-resolution $\delta^{13}C$ stratigraphy through the early Aptian "Livello Selli" of the Alpine Tethys. Paleoceanography. 13, 530-545.

Meyn, H., Vespermann, J., 1994. Taxonomische Revision von Foraminiferen der Unterkreid SE-Niedersachsens nach Roemer (1839, 1841, 1842), Kock (1851) und Reuss (1863). In: Malz, H. (Ed.), Senckenbergiana Lethaea. Senckenbergiana. 74(1-2), 49-272.

Michalík, J., Soták, J., Lintnerová, O., Halásová, E., Bąk, M., Skupien, P., Boorova, D., 2008. The stratigraphic and paleoenvironmental setting of Aptian OAE black shale deposits in the Pieniny Klippen Belt, Slovak Western Carpathians. Cretaceous Res. 29(5-6), 871-892.

Mjatliuk, E. V., 1988. Atlas of Characteristic Foraminifera of the Lower Cretaceous Deposits of the Pre-Caspian Lowlands, Mangyshak Peninsula, and Ustyurt. Nedra Publishers, Leningrad Branch.

262 pp.

Moullade, M., Tronchetti, G., Bellier, J.-P., 2005. The Gargasian (Middle Aptian) strata from Cassis-La Bedoule (Lower Aptian historical stratotype, SE France): Planktonic and benthic foraminiferal assemblages and biostratigraphy. Carnets Geol. 1-20.

Moullade, M., Tronchetti, G., Granier, B., Bornemann, A., Kuhnt, W., Lorenzen, J., 2015. High-resolution integrated stratigraphy of the OAE1a and enclosing strata from core drillings in the Bedoulian stratotype (Roquefort-La Bédoule, SE France). Cretaceous Res. 56. 119-140.

Munsel, D., Kramar, U., Dissard, D., Nehrke, G., Berner, Z., Bijma, J., Neumann, T., 2010. Heavy metal incorporation in foraminiferal calcite: results from multi-element enrichment culture experiments with Ammonia tepida. Biogeosciences. 7(8), 2339-2350.

Munsel, D. M. D., 2013. Utilisation of trace element contents in benthic foraminifera for reconstructing sea water composition. Thesis doctoral. Karlsruher Instituts für Technologie (KIT). Karlsruhe, Germany. 188 pp.

Murray, J. W., Alve, E., 1999. Natural dissolution of modern shallow water benthic foraminifera: taphonomic effects on the palaeoecological record. Palaeogeogr. Palaeoclimatol. Palaeoecol. 146(1-4), 195-209.

Mutterlose, J., Böckel, B., 1998. The Barremian–Aptian interval in NW Germany: a review. Cretaceous Res. 19(5), 539-568.

Mutterlose, J., Bottini, C., Schouten, S., Sinninghe Damsté, J. S., 2014. High sea-surface temperatures during the early Aptian Oceanic Anoxic Event 1a in the Boreal Realm. Geology. 42(5), 439-442.

Naafs, B. D. A., Pancost, R. D., 2016. Sea-surface temperature evolution across Aptian oceanic anoxic event 1a. Geology. 44(11), 959-962.

Nagy, J., Gradstein, F. M., Gibling, M. R., Thomas, F. C., 1995. Foraminiferal stratigraphy and paleoenvironments of Late Jurassic to Early Cretaceous deposits in Thakkhola, Nepal. Micropaleontology. 41(2), 143-170.

Nyong, E. E., Olsson, R. K., 1984. A paleoslope model of Campanian to Lower Maestrichtian foraminifera in the North American basin and adjacent continental margin. Mar. Micropaleontol. 8(6), 437-477.

Pancost, R. D., Crawford, N., Magness, S., Turner, A., Jenkyns, H. C., Maxwell, J. R., 2004, Further evidence for the development of photic-zone euxinic conditions during Mesozoic oceanic anoxic events. Geol Soc London. 161, 353-364.

Patruno, S., Triantaphyllou, M. V., Erba, E., Dimiza, M. D., Bottini, C., Kaminski, M. A., 2015. The Barremian and Aptian stepwise development of the 'Oceanic Anoxic Event 1a' (OAE 1a) crisis: Integrated benthic and planktic high-resolution palaeoecology along the Gorgo a Cerbara stratotype section (Umbria–Marche Basin, Italy). Palaeogeogr. Palaeoclimatol. Palaeoecol. 424, 147-182.

Percival, L. M. E., Tedeschi, L. R., Creaser, R. A., Bottini, C., Erba, E., Giraud, F., Jenkyns, H. C., 2021. Determining the style and provenance of magmatic activity during the Early Aptian Oceanic Anoxic Event (OAE 1a). Global and Planetary Change. 103461.

Piña-Ochoa, E., Høgslund, S., Geslin, E., Cedhagen, T., Revsbech, N. P., Nielsen, L. P., .Risgaard-Petersen, N., 2010. Widespread occurrence of nitrate storage and denitrification among Foraminifera and Gromiida. PNAS. 107(3), 1148-1153.

Premoli Silva, I., Erba, E., Salvini, G., Verga, D., Locatelli, C., 1999. Biotic changes in Cretaceous anoxic events J. Foraminiferal Res. 29, 352-370.

Price, G.D., 2003. New constraints upon isotope variation during the Early Cretaceous (Barremian–Cenomanian) from the Pacific Ocean. Geol. Mag. 140, 513-522.

Quan, T. M., Wright, J. D., Falkowski, P. G., 2013. Co-variation of nitrogen isotopes and redox states through glacial–interglacial cycles in the Black Sea. Geochim Cosmochim Ac. 112, 305-320.

Reolid, M., Martínez-Ruiz, F., 2012. Comparison of benthic foraminifera and geochemical proxies in shelf deposits from the Upper Jurassic of the Prebetic (southern Spain). J. Iber. Geol. 38(2), 449-465.

Reolid, M., Rodríguez-Tovar, F. J., Nagy, J., Olóriz, F., 2008. Benthic foraminiferal morphogroups of mid to outer shelf environments of the Late Jurassic (Prebetic Zone, southern Spain): characterization of biofacies and environmental significance. Palaeogeogr. Palaeoclimatol. Palaeoecol. 261 (3-4), 280-299.

Riegraf, W., 1989. Benthonische Schelf-Foraminiferen aus dem Valanginium-Hauterivium (Unterkreide) des Indischen Ozeans südwestlich Madagaskar (Deep Sea Drilling Project Leg 25, Site 249). Geol Rundsch. 78(3), 1047-1061.

Risgaard-Petersen, N., Langezaal, A. M., Ingvardsen, S., Schmid, M. C., Jetten, M. S., den Camp, H. J. O., Revsbech, N. P., 2006. Evidence for complete denitrification in a benthic foraminifer. Nature. 443(7107), 93-96.

Robinson, S. A., Heimhofer, U., Hesselbo, S. P., Petrizzo, M. R., 2017. Mesozoic climates and oceans–a tribute to Hugh Jenkyns and Helmut Weissert. Sedimentology. 64(1), 1-15.

Rückheim, S., Bornemann, A., Mutterlose, J., 2006. Integrated stratigraphy of an Early Cretaceous (Barremian–Early Albian) North Sea borehole (BGS 81/40). Cretaceous Res. 27(3), 447-463.

Saint-Marc, P., 1992. Biogeographic and bathymetric distribution of benthic foraminifera in Paleocene El Haria Formation of Tunisia J. Afr. Earth Sci. 15(3-4), 473-487.

Schlanger, S. O., Jenkyns, H. C., 1976. Cretaceous oceanic anoxic events: causes and consequences. Geol Mijnbouw. 55(3-4), 179-184.

Schlanger, S. O., Arthur, M. A., Jenkyns, H. C., Scholle, P. A., 1987. The Cenomanian-Turonian Oceanic Anoxic Event, I. Stratigraphy and distribution of organic carbon-rich beds and the marine $\delta^{13}C$ excursion. Geol. Soc. Spec. Publ. 26(1), 371-399.

Schnack, K., 2000. Biostratigraphie und fazielle Entwicklung in der Oberkreide und im Alttertiär im Bereich der Kharga Schwelle, Westliche Wüste, southwest Ägypten: Ph.D. Thesis Nr. 151. Universität Bremen, Bremen, Germany. 142 pp.

Schneider-Mor, A., Alsenz, H., Ashckenazi-Polivoda, S., Illner, P., Abramovich, S., Feinstein, S., Püttmann, W., 2012. Paleoceanographic reconstruction of the late Cretaceous oil shale of the Negev, Israel: Integration of geochemical, and stable isotope records of the organic matter. Palaeogeogr. Palaeoclimatol. Palaeoecol. 319, 46-57.

Shannon, C. E., Weaver, W., 1949. The Mathematical Theory of Communication: University of Illinois Press, Urbana. 125 pp.

Sliter, W. V., Baker, R. A., 1972. Cretaceous bathymetric distribution of benthic foraminifers. J. Foraminiferal Res. 2(4), 167-183.

Stein, M., Föllmi, K.B., Westermann, S., Godet, A., Adatte, T., Matera, V., Fleitmann, D., Berner, Z., 2011. Progressive palaeoenvironmental change during the late Barremian–early Aptian as prelude to Oceanic Anoxic Event 1a: Evidence from the Gorgo a Cerbara section (Umbria-Marche basin, central Italy). Palaeogeogr. Palaeoclimatol. Palaeoecol. 302, 396-406.

Suchéras-Marx, B., Escarguel, G., Ferreira, J., Hammer, Ø., 2019. Statistical confidence intervals for relative abundances and abundance-based ratios: Simple practical solutions for an old overlooked question. Mar. Micropaleontol. 151, 1-6.

Szarek, R., Osowska, B. K., Prokoph, A., Kuhnt, W., Wagner, T., 2000. Upper Albian agglutinated foraminifera from two wells in Northeast Germany. Grzyb Found Spec Pub. 3, 141-144.

Szydło, A., (2004). The distribution of agglutinated foraminifera in the Cieszyn Basin, Polish Outer Carpathians. Grzyb Found Spec Pub. 8, 461-470.

Tejada, M. L. G., Katsuhiko, S., Kuroda, J., Coccioni, R., Mahoney, J. J., Ohkouchi, N., Sakamoto, T., Tatsumi, Y., 2009. Ontong Java Plateau eruption as a trigger for the early Aptian oceanic anoxic event. Geology. 37, 855-858,

Tyszka, J., 1994. Response of Middle Jurassic benthic foraminiferal morphogroups to dysoxic/anoxic conditions in the Pieniny Klippen Basin, Polish Carpathians. Palaeogeogr. Palaeoclimatol. Palaeoecol. 110 (1-2), 55-81.

Tyszka, J., 2006. Taxonomy of Albian Gavelinellidae (Foraminifera) from the Lower Saxony Basin, Germany. Palaeontology. 49(6), 1303-1334.

van Breugel, Y., Schouten, S., Tsikos, H., Erba, E., Price, G. D., Sinninghe Damsté, J. S., 2007. Synchronous negative carbon isotope shifts in marine and terrestrial biomarkers at the onset of the early Aptian oceanic anoxic event 1a: Evidence for the release of ^{13}C-depleted carbon into the atmosphere. Paleoceanography. 22, 1-13.

van Den Akker, T. J. H. A., Kaminski, M. A., Gradstein, F. M., Wood, J., 2000. Campanian to Palaeocene biostratigraphy and palaeoenvironments in the Foula Sub-basin, west of the Shetland Islands, UK. J Micropalaeontol. 19(1), 23-43.

van der Zwaan, G. J., Duijnstee, I. A. P., Den Dulk, M., Ernst, S. R., Jannink, N. T., Kouwenhoven, T. J., 1999. Benthic foraminifers: proxies or problems?: a review of paleocological concepts. Earth-Sci. Rev. 46 (1-4), 213-236.

van Morkhoven, F. P., Berggren, W. A., Edwards, A. S., Oertli, H. J., 1986, Cenozoic cosmopolitan deep-water benthic foraminifera: Bulletin des Centres de Recherches Exploration-Production Elf-Aquitaine, Pau. 421 pp.

Verga, D., Premoli Silva, I., 2002. Early Cretaceous planktonic foraminifera from the Tethys: the genus Leupoldina. Cretaceous Res. 23, 189-212.

Verga, D., Premoli Silva, I., 2003a. Early Cretaceous planktonic foraminifera from the Tethys: the small, few-chambered representatives of the genus Globigerinelloides. Cretaceous Res. 24, 305-334.

Verga, D., Premoli Silva, I., 2003b. Early Cretaceous planktonic foraminifera from the Tethys: the large-sized, many-chambered representatives of the genus Globigerinelloides. Cretaceous Res. 24, 661-690.

Verga, D., Premoli Silva, I., 2005. Early Cretaceous planktonic foraminifera from the Tethys: the upper Aptian, planispiral morphotypes with elongate chambers. Cretaceous Res. 26, 239-259.

von Bargen, D., Lehmann, J., 2014. Benthic ecosystem response to the deposition of lower Aptian black shales in an epicontinental sea. Cretaceous Res. 51, 208-224.

Weidich, K. F., 1990. Die kalkalpine Unterkreide und ihre Foraminiferen fauna. Zitteliana. Zitteliana, 17, 3-312.

Weissert, H., 1989. C-isotope stratigraphy, a monitor of paleoenvironmental changes: A case study from the Early Cretaceous. Surv. Geophys. 10, 1-61.

Weissert, H., 1990. Siliciclastics in the Early Cretaceous Tethys and North Atlantic Oceans: Documents of periodic greenhouse climate conditions. Mem. Soc. Geol. Ital. 44, 59-69.

Weissert, H., Lini, A., 1991, Ice Age interludes during the time of Cretaceous greenhouse climate?, in Müller, D.W., McKenzie, J.A., and Weissert, H., eds., Controversies in Modern Geology. San Diego, California, Academic Press. p. 173-191.

Weissert, H., Erba, E., 2004. Volcanism, CO2 and palaeoclimate: a Late Jurassic–Early Cretaceous carbon and oxygen isotope record. J Geol Soc. 161(4), 695-702.

Wissler, L., Funk, H., Weissert, H., 2003. Response of Early Cretaceous carbonate platforms to changes in atmospheric carbon dioxide levels. Palaeogeogr. Palaeoclimatol. Palaeoecol. 200(1-4), 187-205.

Zorina, S. O., Pavlova, O. V., Galiullin, B. M., Morozov, V. P., Eskin, A. A., 2017. Euxinia as a dominant process during OAE1a (Early Aptian) on the Eastern Russian Platform and during OAE1b (Early Albian) in the Middle Caspian. Sci. China Earth Sci. 60(1), 58-70.

Appendix A

Taxonomic appendix

Taxonomic list of the benthic foraminifera taxa cited in the text is based on Ellis and Messina (1940-2015), Mjatliuk (1988), Weidich (1990), Meyn and Vespermann (1994), Holbourn and Kaminski (1997), Patruno et al. (2015).

Agglutinated foraminifera:

Ammobaculites sp. Cushman, 1910

Ammodiscus sp. Reuss, 1862

Ammodiscus cretaceus (Reuss, 1845)

Ammodiscus infimus Franke, 1936

Bathysiphon sp. Sars, 1872

Bathysiphon brosgei Tappan, 1957

Bathysiphon vitta Nauss, 1947

Bimonilina Eicher, 1960

Bimonilina entis Mjatliuk, 1988

Dorothia sp. Plummer, 1931

Dorothia hyperconica Risch, 1970

Gaudryina sp. d'Orbigny, 1839

Gaudryina dividens Grabert, 1959

Glomospira sp. Rzehak, 1885

Glomospira gordialis (Jones and Parker, 1860)

Glomospira charoides (Jones and Parker, 1860).

Glomospirella sp. Plummer, 1945

Haplophragmoides sp. Cushman, 1910

Haplophragmoides kirki Wickenden, 1932

Haplophragmoides gigas gigas Cushman, 1927

Haplophragmoides gigas minor Nauss, 1947

Hippocrepina Parker, 1870

Hippocrepina depressa Vašíček, 1947

Reophax sp. Montfort, 1808

Reophax helveticus (Haeusler, 1881)

Reophax liasicus Franke, 1936

Rhizammina sp. Brady, 1879

Scherochorella Loeblich and Tappan, 1984

Scherochorella minuta Tappan, 1940 = *Reophax minutus* Tappan, 1940

Spiroplectinata sp. Cushman, 1927

Spiroplectinata lata Grabert, 1959

Tolypammina sp. Rhumbler, 1895

Tritaxia Reuss, 1860

Tritaxia pyramidata Reuss, 1863

Verneuilinoides sp. Loeblich & Tappan, 1949

Verneuilinoides cf. *neocomiensis* (Mjatliuk, 1939)

Calcareous foraminifera:

Astacolus sp. Montfort, 1808

Astacolus calliopsis (Reuss, 1863)

Astacolus humilis (Reuss, 1863)

Astacolus planiusculus (Reuss, 1863).

Dentalina sp. Risso, 1826

Dentalina comunis (d'Orbigny, 1826) = *Laevidentalina comunis* (d'Orbigny, 1826)

Dentalina gracilis d'Orbigny, 1840

Dentalina guttifera (d'Orbigny, 1846) = *Laevidentalina guttifera* (d'Orbigny, 1846)

Gavelinella sp. Brotzen, 1942

Gavelinella barremiana Bettenstaedt, 1952

Gavelinella berthelini Fuchs, 1967

Gavelinella intermedia intermedia = Berthelina intermedia (Berthelin, 1880)

Globulina sp. d'Orbigny, 1839

Globulina prisca (Reuss, 1863)

Guttulina sp. d'Orbigny, 1839

Gyroidina sp. d'Orbigny, 1826

    Gyroidina globosa (Hagenow 1842) = *Gyroidinoides globosa* (Hagenow 1842)

    Gyroidina nitida (Reuss, 1850) = *Gyroidinoides nitida* (Reuss, 1844)

    Laevidentalina sp. Loeblich & Tappan, 1986

    Laevidentalina distincta (Reuss, 1960) = *Dentalina distincta* (Reuss, 1860)

    Laevidentalina linearis (Roemer, 1841)

    Laevidentalina soluta (Reuss, 1851)

Lenticulina sp. Lamarck, 1804

    Lenticulina macrodisca (Reuss, 1863)

    Lenticulina muensteri (Roemer, 1839)

    Lenticulina pulchella (Reuss, 1863)

    Lenticulina subgaultina Bartenstein, 1962

    Lenticulina turgidula (Reuss, 1863)

Lingulonodosaria Silvestri, 1903

Lingulonodosaria nodosaria (Reuss, 1863)

Lingulina sp. d'Orbigny, 1826

Nodosaria sp. Lamarck, 1816

Pleurostomella sp. Reuss, 1860

    Pleurostomella reussi Berthelin, 1880 = *Pleurostomella subnodosa* (Reuss, 1851)

Pseudonodosaria sp. Boomgaart, 1949

    Pseudonodosaria humilis (Roemer, 1841)

Pyrulina sp. d'Orbigny, 1839

Saracenaria sp. Defrance, 1824

    Saracenaria sp1.

Saracenaria sp2.

Stilostomella sp. Guppy, 1894

Vaginulinopsis sp. Silvestri, 1904

Figures

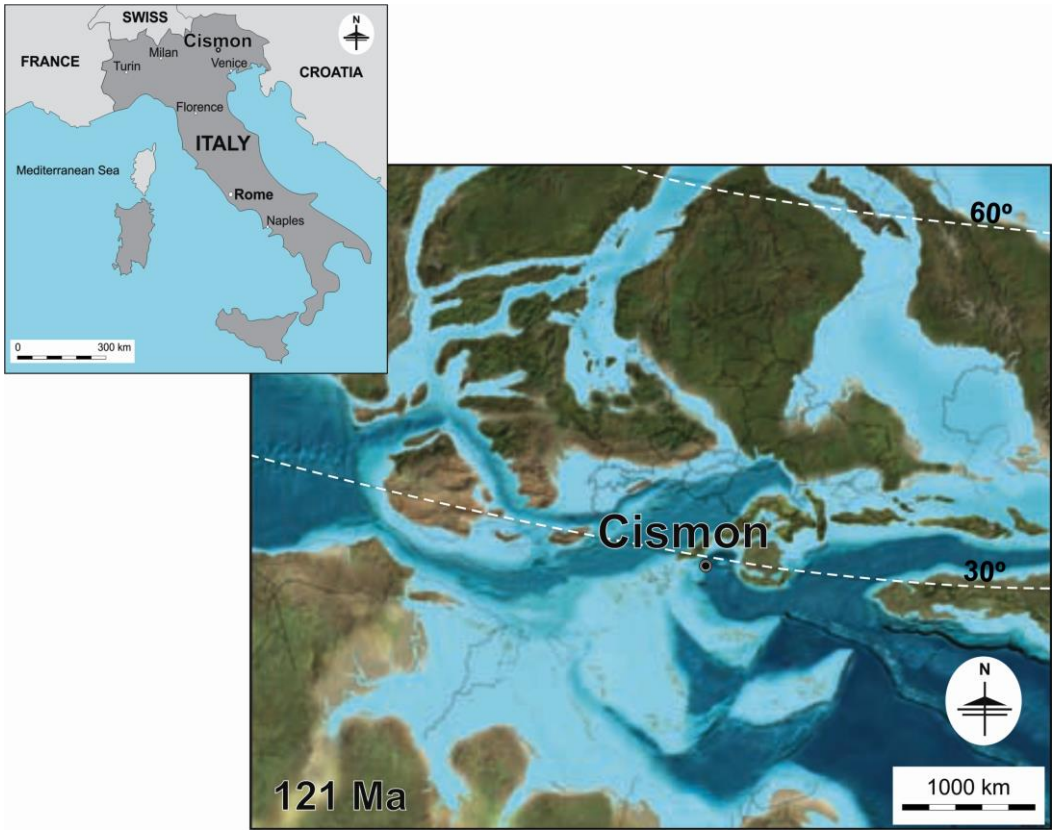

Fig. 1. Location of the Cismon today (upper left) and in the early Aptian (ca. 121 Ma). Paleogeographical map of the western Tethys modified from Blakey (2012), NAU Geology. http://jan.ucc.nau.edu/~rcb7/.

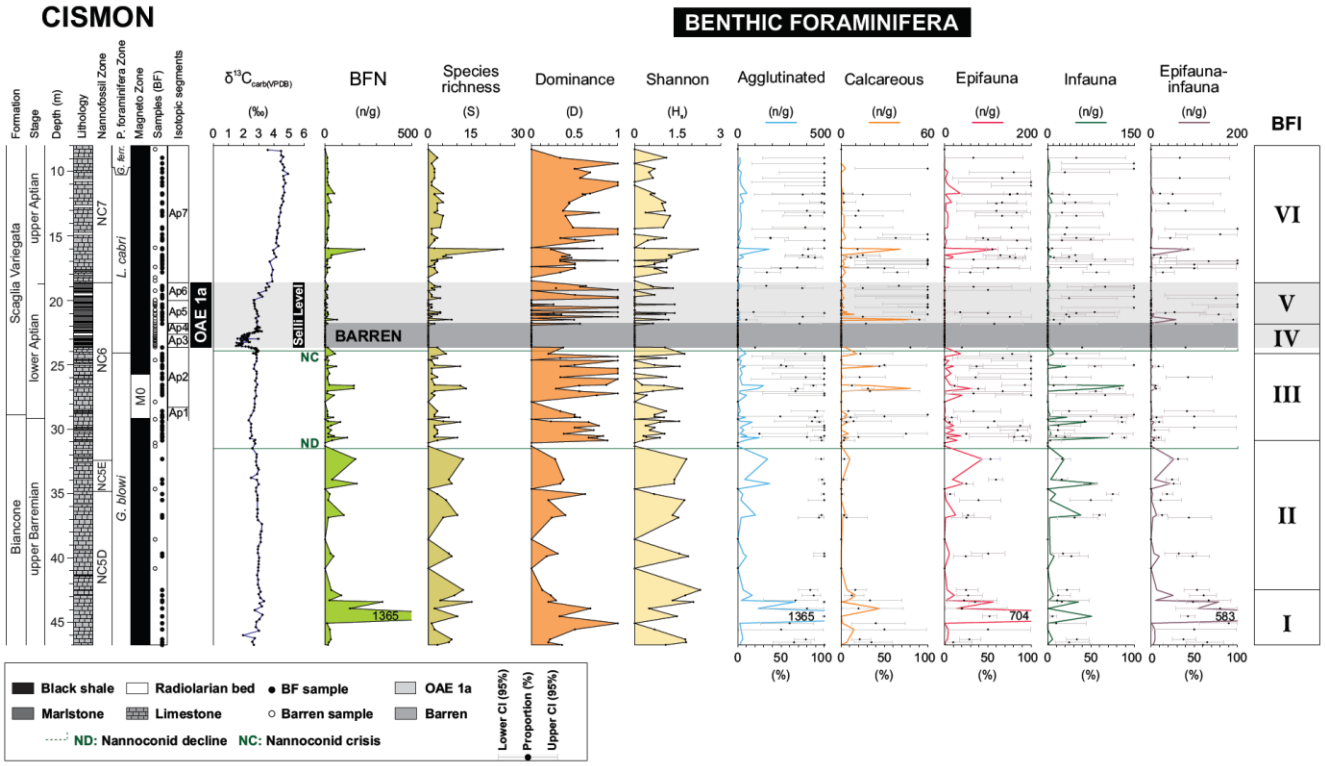

Fig. 2. Benthic foraminifera distribution in the upper Barremian-upper Aptian interval of the Cismon Core. The benthic foraminifera number (BFN), species richness (S), Shannon index (H_S), Dominance (D), confidence interval (CI%), relative (%), and absolute (number of specimens per gram of washed residue = n/g) abundances of the agglutinated foraminifera, calcareous foraminifera, epifauna and infauna morphogroups, and epifauna-infauna are reported. The Benthic Foraminifera Intervals (BFI) identified in this work are displayed. Lithology, planktonic foraminifera, and nannofossil biostratigraphy are after Erba et al. (1999) and Bottini et al. (2015). ND = nannoconid decline at 31.50 m; NC = nannoconid crisis at 23.90 m. Magnetostratigraphy is from Channell et al. (2000). $\delta^{13}C_{carb}$ data are from Erba et al. (1999) and Méhay et al. (2009). The isotopic segments Ap1-Ap7 are after Bottini et al. (2015). TOC is after Erba et al. (1999) and Bottini et al. (2012).

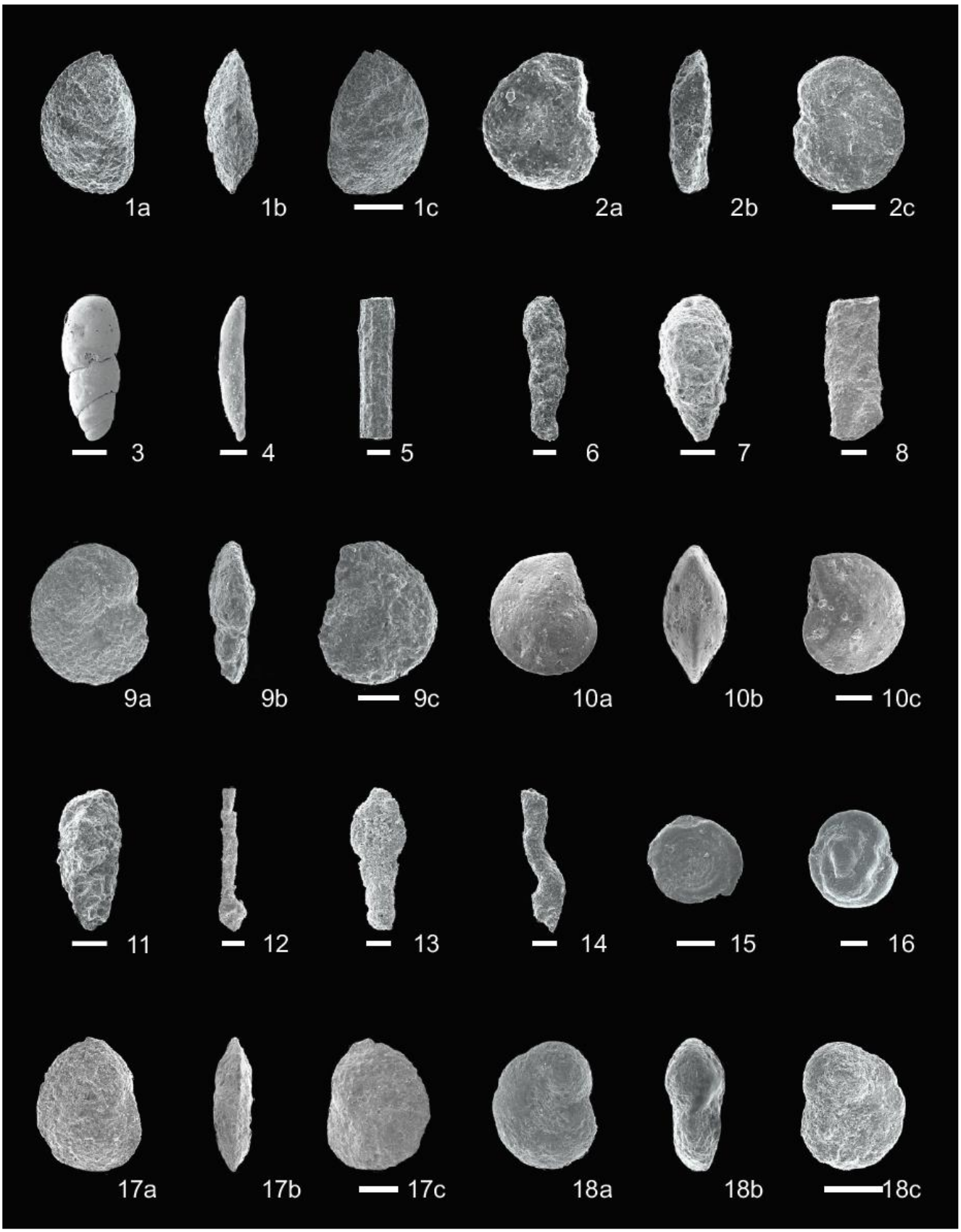
1a
1b
1c
2a
2b
2c
3
4
5
6
7
8
9a
9b
9c
10a
10b
10c
11
12
13
14
15
16
17a
17b
17c
18a
18b
18c

1380

Fig. 3. Benthic foraminifera of the Cismon Core. Scale-bars are 100 μm. **1.** a/b/c *Astacolus planiusculus* (core 12 – 12/162; 15.98 m); **2.** *Gavelinella* sp.(core 12 – 12/162; 15.98 m); **3.** *Lingulonodosaria nodosaria* (core 13 – Rad 35; 17.78 m); **4.** *Laevidentalina soluta* (core 13 – Rad 35; 17.78 m); **5.** *Bathysiphon brosgei* (core 12 – 12/162; 15.98 m); **6.** *Scherochorella minuta* (core 162 – 16/99; 26.82 m); **7.** *Dorothia hyperconica* (core 17 – 17/211; 30.63 m); **8.** *Rhizammina* sp. (core 23 – 23/38; 44.53 m); **9.** a/b/c *Gavelinella barremiana* (core 12 – 12/162; 15.98 m); **10.** a/b/c *Lenticulina muensteri* (core 14 – 14/167; 21.46 m); **11.** *Bimonilina entis* (core 16 – 16/79; 30.63 m); **12.** *Tolypammina* sp. (core 14 – Rad 53; 21.23 m); **13.** *Reophax helveticus* (core 15 – Rad 75; 24.12 m); **14.** *Rhizammina* sp. (core 12 – 12/162; 15.98 m); **15.** *Ammodiscus cretaceus* (core 12 – 12/162; 15.98 m); **16.** *Glomospira charoides* (core 12 – 12/162; 15.98 m); **17.** a/b/c *Astacolus calliopsis* (core 12 – 12/162; 15.98 m); **18.** a/b/c *Gavelinella intermedia* (core 15 – 15/124; 25.09 m).

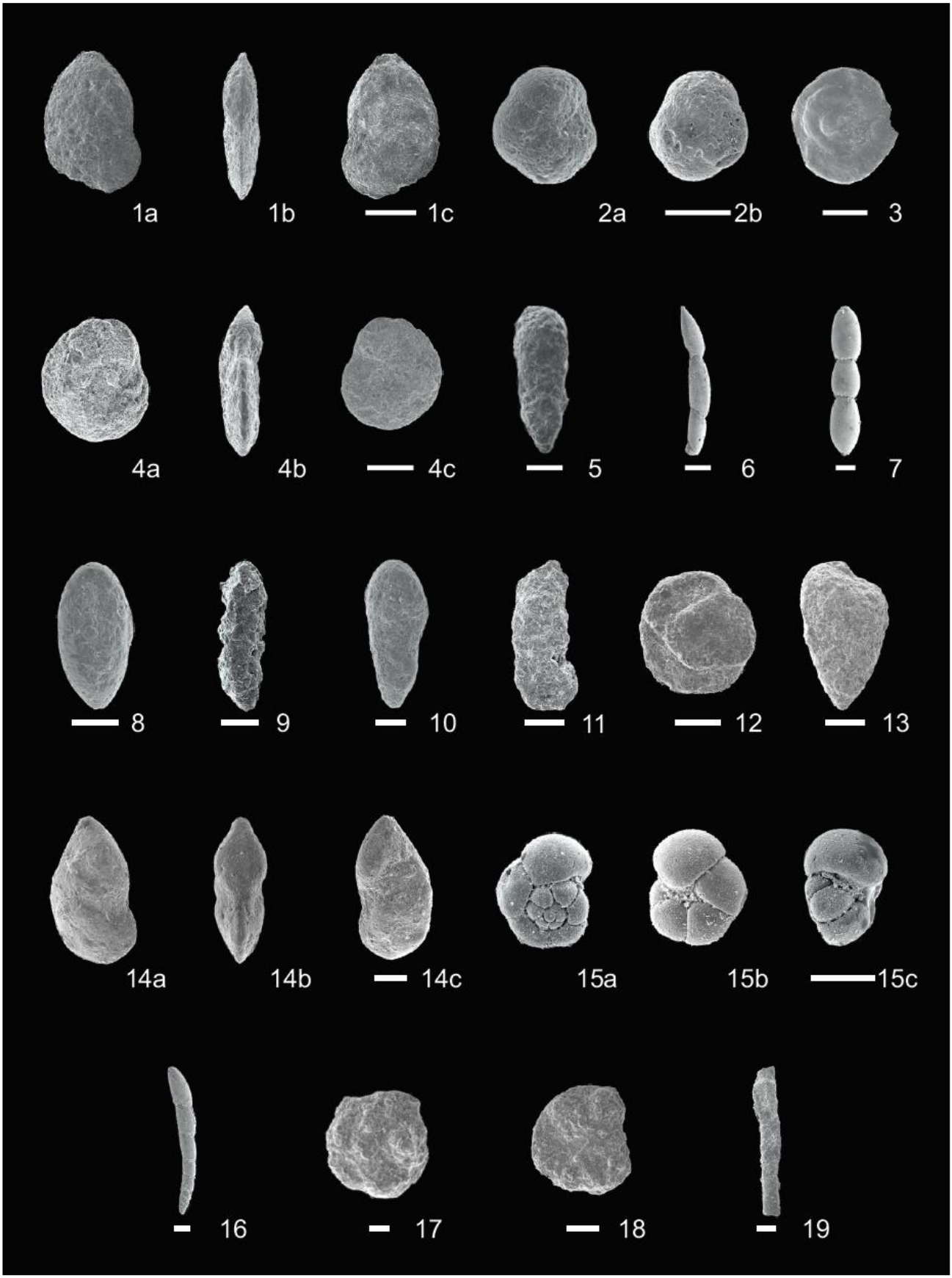
1a
1b
1c
2a
2b
3
4a
4b
4c
5
6
7
8
9
10
11
12
13
14a
14b
14c
15a
15b
15c
16
17
18
19

1407

Fig. 4. Benthic foraminifera of the Cismon Core. Scale-bars are 100 μm. **1.** a/b/c *Lenticulina subgaultina* (core 12 – 12/162; 15.98 m); **2.** a/b *Gyroidina globosa* (core 15 – 15/124; 25.09 m); **3.** *Glomospira gordialis* (core 12 – 12/162; 15.98 m); **4.** a/b/c *Gavelinella barremiana* (core 16 – 16/98; 26.82 m); **5.** *Verneuilinoides cf. neocomiensis* (core 17 – 17/211; 30.63 m); **6.** *Laevidentalina distincta* (core 13 – Rad 35; 17.78 m); **7.** *Pleurostomella reussi* (core 14 – Rad 50; 20.87 m); **8.** *Globulina prisca* (core 15 – 15/124; 25.09 m); **9.** *Verneuilinoides* sp. (core 17 – 17/211; 30.63 m); **10.** *Verneuilinoides* cf. *neocomiensis* (core 15 – 15/124; 25.09 m); **11.** *Reophax liasicus* (core 18 – 18/265; 33.89 m); **12.** *Haplophragmoides kirki* (core 22 – 22/224; 21.23 m); **13.** *Dorothia hyperconica* (core 16 – 16/79; 42.90 m); **14.** a/b/c *Vaginulinopsis* sp. (core 1 – 14/167W; 21.46 m); **15.** a/b/c *Gyroidina nitida* (core 12 – Rad 27; 16.78 m); **16.** *Dentalina gracilis* (core 16 – 16/79; 26.59 m); **17.** *Haplophragmoides gigas minor* (core 22 – 22/170; 33.89 m); **18.** *Haplophragmoides gigas gigas* (core 22 – 22/224; 43.41 m); **19.** *Bathysiphon vitta* (core 11 – Rad 16; 14.29 m).

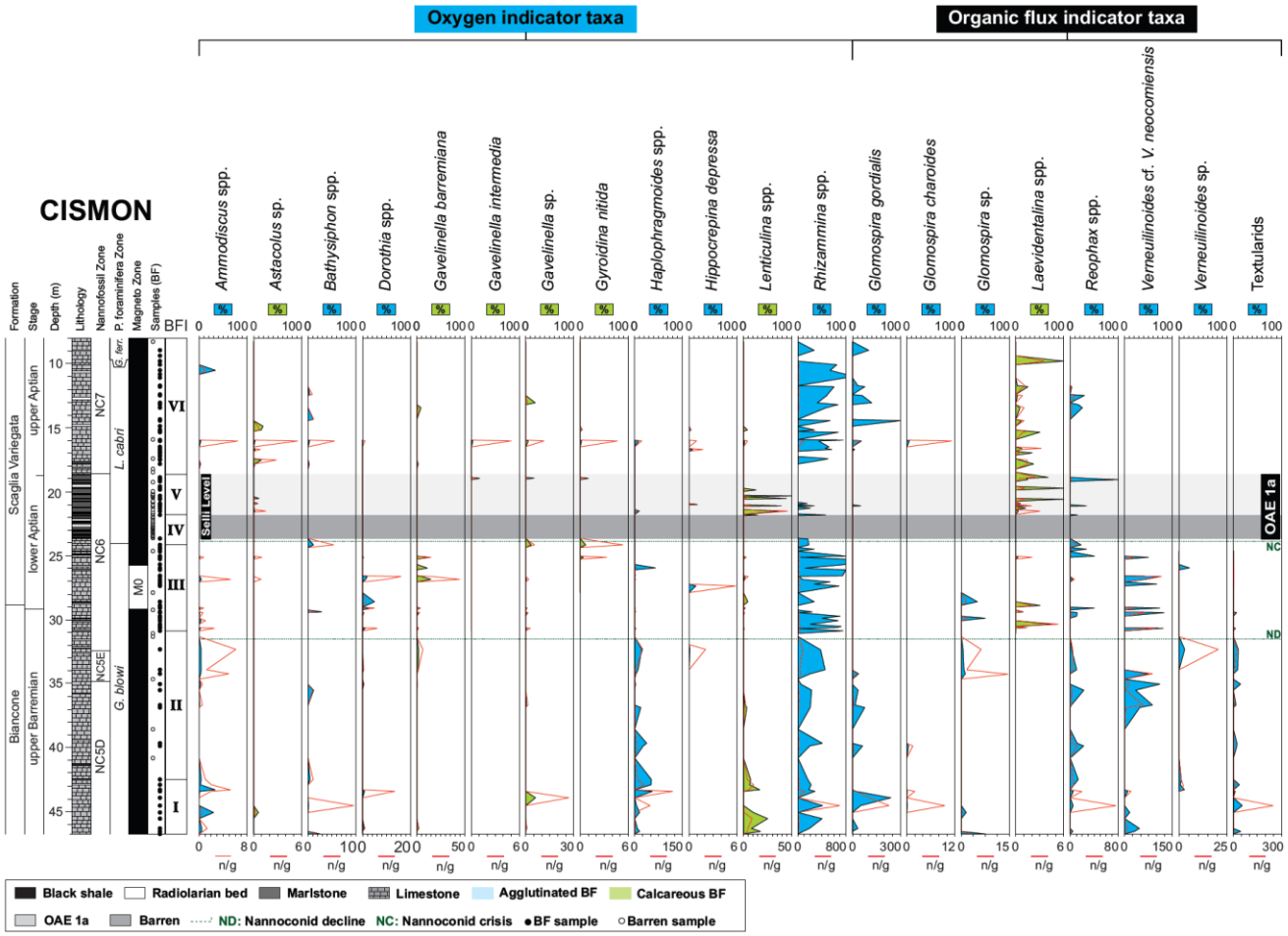

Fig. 5. Relative (%) and absolute (number of specimens per gram of washed residue = n/g) abundances of the most common benthic foraminiferal taxa (grouped at genus level) identified in the Cismon Core. BFI = Benthic foraminifera intervals. Lithology, planktonic foraminifera, and nannofossil biostratigraphy are after Erba et al. (1999) and Bottini et al. (2015). ND = nannoconid decline at 31.50 m; NC = nannoconid crisis at 23.90 m. Magnetostratigraphy is from Channell et al. (2000).

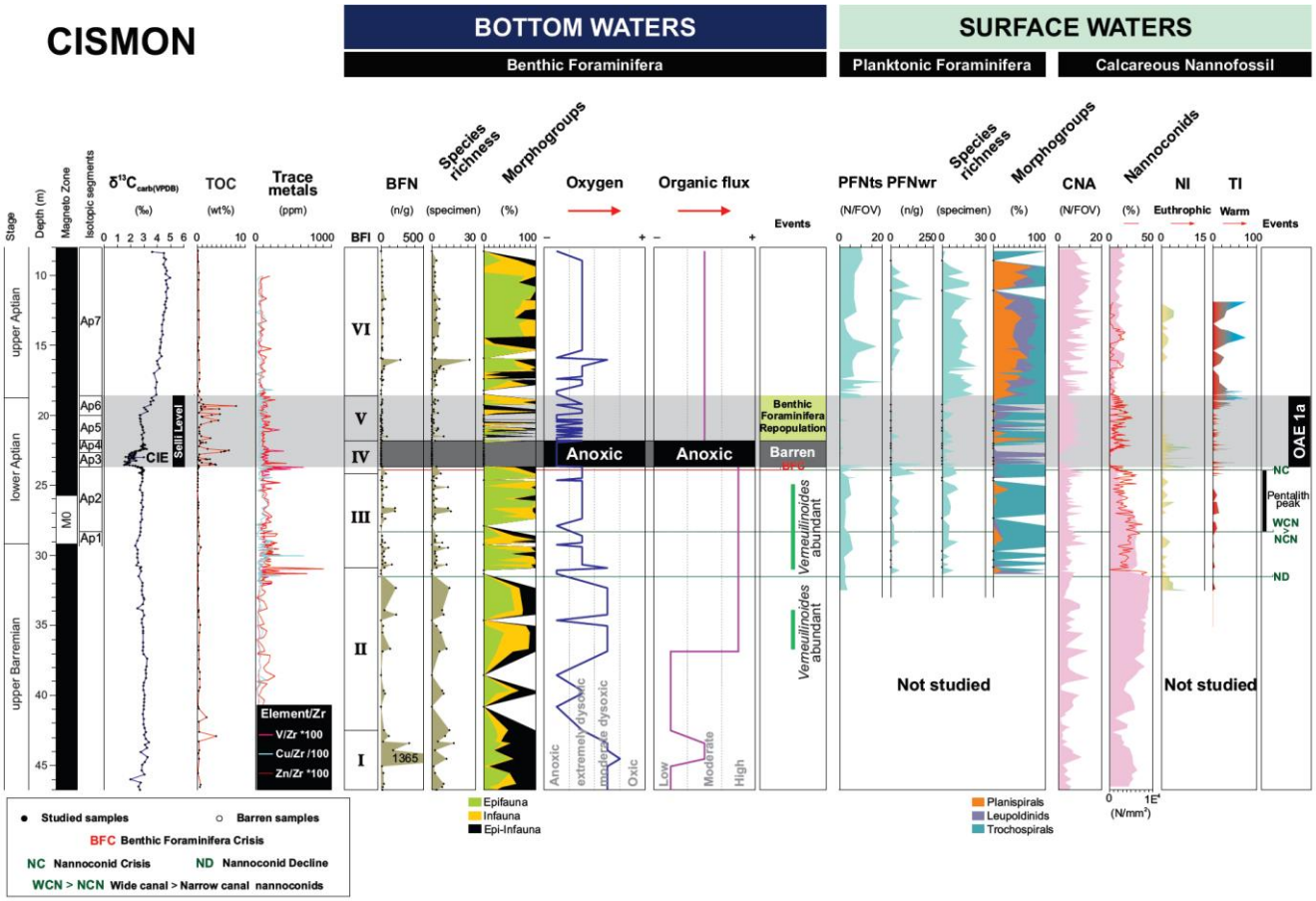

Fig. 6. Paleoenvironmental interpretation of the bottom-water and surface-water conditions based on benthic foraminifera (this study), calcareous nannofossils (Erba and Tremolada, 2004; Erba et al., 2010; Bottini et al., 2015) and planktonic foraminifera (Barchetta, 2015; this study) through the upper Barremian-lower upper Aptian sedimentary sequence in the Cismon Core. Paleoenvironmental interpretation of bottom-water conditions based on benthic foraminiferal assemblages (this work). Magnetostratigraphy is from Channell et al. (2000). $\delta^{13}C_{carb}$ data are after Erba et al. (1999) and Méhay et al. (2009). The isotopic segments Ap1-Ap7 are after Bottini et al. (2015). TOC is after Erba et al. (1999) and Bottini et al. (2012). Trace metal abundances are after Erba et al. (2015). The Nannofossil Nutrient Index (NI) and Temperature Index (TI) are from Bottini et al. (2015). BFI = Benthic Foraminifera Intervals; BFN = benthic foraminifera absolute abundance; PFNwr = planktonic foraminifera absolute abundance in washed residues n/40 field of view; n/g = number of specimens per gram of washed residue; PFNts = planktonic foraminifera absolute abundance in thin sections; CNA = calcareous nannofossils abundance; N/FOV = number of specimens per fields of view; ND =

nannoconid decline at 31.50 m; NCN = narrow canal nannoconids; WCN= wide canal nannoconids; NC = nannoconid crisis at 23.90 m; BFC = benthic foraminifera crisis at 23.89 m.

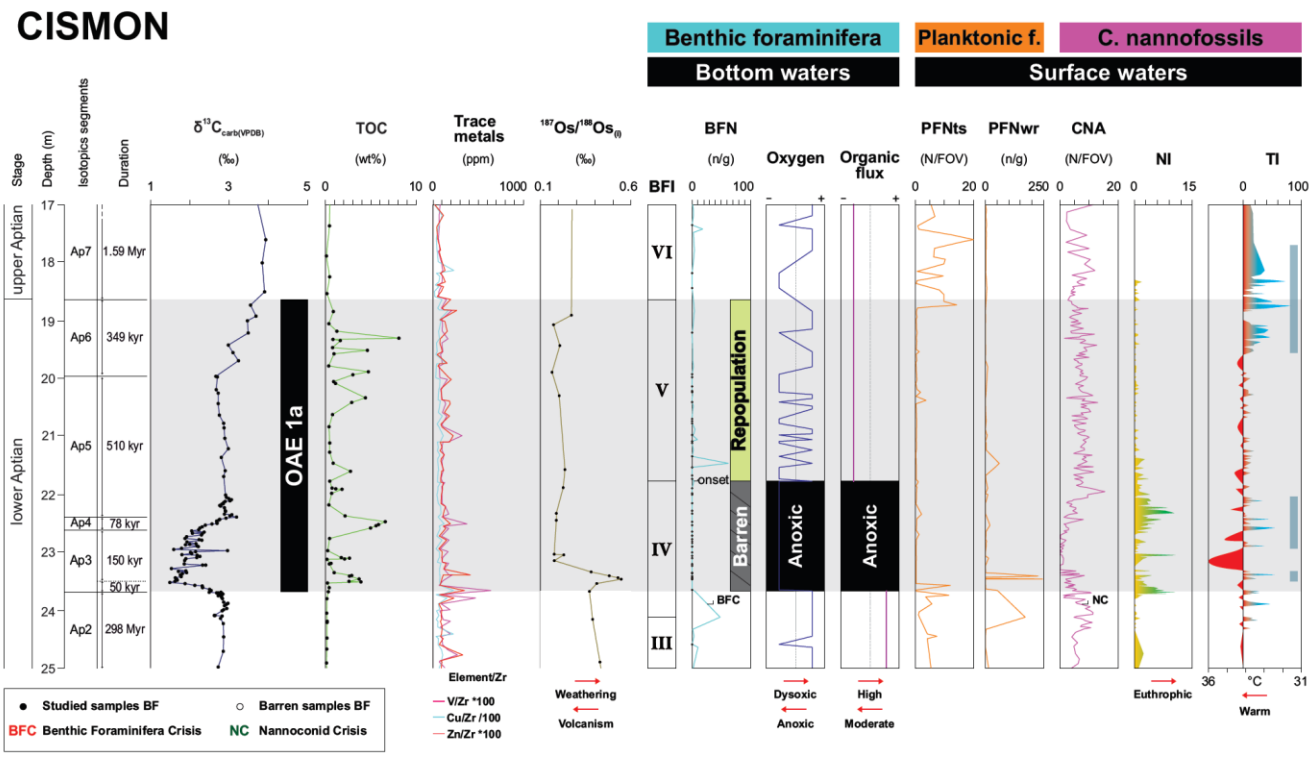

Fig. 7. OAE 1a closeup in the Cismon Core. $\delta^{13}C_{carb}$ data are after Erba et al. (1999) and Méhay et al. (2009). The isotopic segments Ap2-Ap7 after Bottini et al. (2015). Duration of the isotopic segments according to Malinverno et al. (2010). TOC is after Erba et al. (1999) and Bottini et al. (2012). Trace metal abundances are from Erba et al. (2015). The Os-isotope curve is after Bottini et al. (2012). Benthic foraminiferal data (oxygen, organic flux) are from this study. Planktonic foraminiferal data are after Barchetta (2015) and this study. Calcareous nannofossil data are after Erba et al. (1999) and Bottini et al. (2015). The Nannofossil Nutrient Index (NI) and Temperature Index (TI) are from Bottini et al. (2015). BFI = Benthic Foraminifera Intervals; BFN = benthic foraminifera absolute abundance; PFNwr = planktonic foraminifera absolute abundance in washed residues, n/g = number of specimens per gram of washed residue; PFNts = planktonic foraminifera absolute abundance in thin sections; CNA = calcareous nannofossils abundance; N/FOV = number of specimens per fields of view; NC = nannoconids crisis at 23.90 m, BFC = benthic foraminifera crisis at 23.89 m.

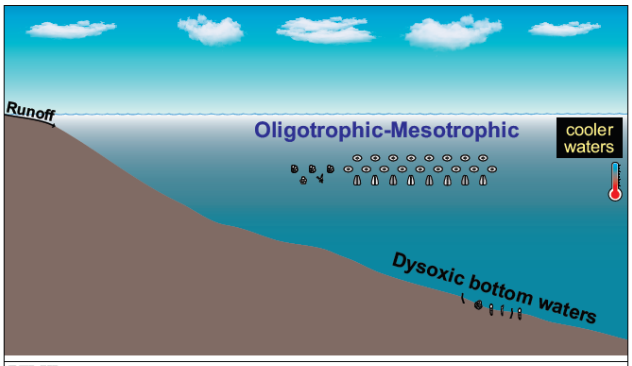

BFI-VI

- low pCO_2
- lower runoff
- sporadic bottom-water ventilation (BF)
- moderate organic flux (BF)

post-OAE 1a

Benthic foraminifera (BF)

- Bathysiphon
- Glomospira
- Lenticulina
- Laevidentalina
- *Pleurostomella*
- *Rhizammina*
- *Verneuilinoides*

Planktonic foraminifera (PK)

- Planispiral
- Trochospiral
- Pseudo-planispiral

Calcareous nannofossils

- Coccoliths
- Narrow-canal Nannoconids
- Wide-canal Nannoconids

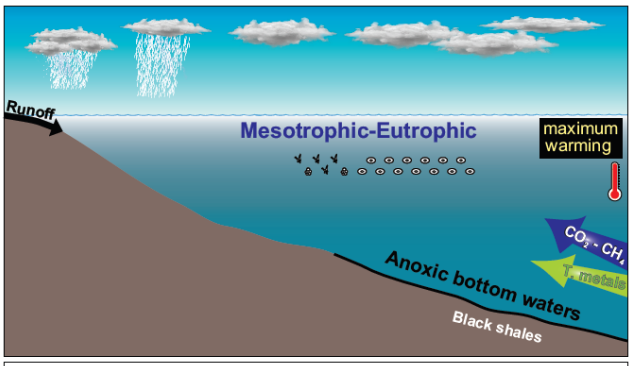

BFI- IV

- high pCO_2
- major injection of volcanogenic CO_2
- increased runoff and precipitation
- black shales depositions
- anoxic bottom-waters (BF)
- surface-water oceanic acidification

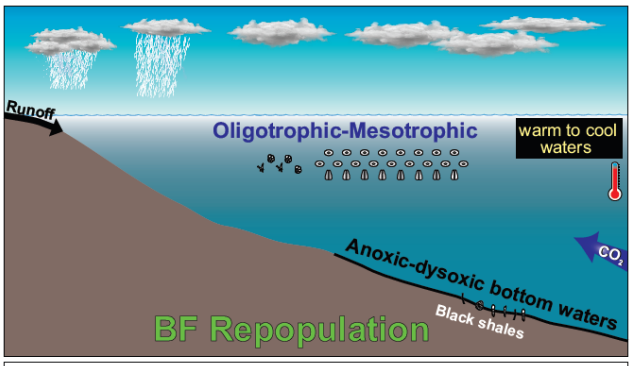

BFI- V

- high pCO_2
- injection of volcanogenic CO_2
- increased runoff and precipitation
- black shales deposits
- sporadic bottom-water ventilation (BF)
- moderate organic flux (BF)

OAE 1a

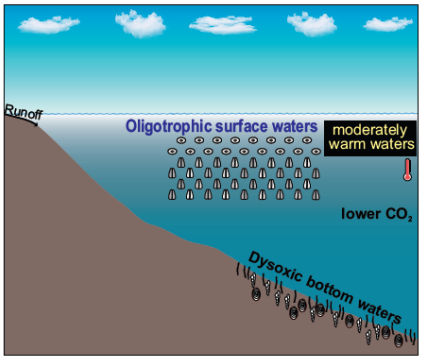

BFI-II

- low pCO_2
- lower runoff
- sporadic bottom-water ventilation (BF)
- high organic flux (BF)
- oxgenated surface-waters (CN)

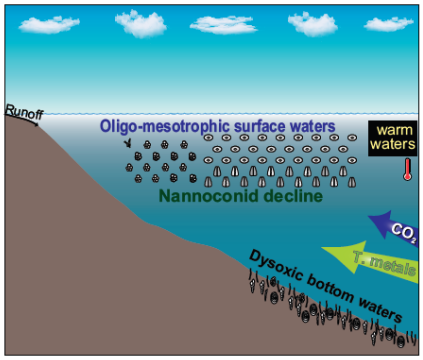

BFI- II and III

- injection of volcanogenic CO_2
- increasing of trace metals (Pb and Cu)
- lower runoff
- sporadic bottom-water ventilation (BF)
- high organic flux (BF)
- expanded OMZ

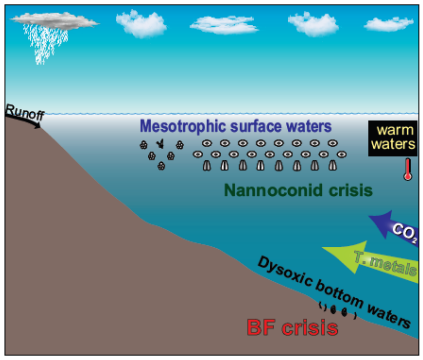

BFI- IV (base)

- low pCO_2
- higher injection of volcanogenic CO_2
- runoff and precipitation increase
- dysoxic bottom-water (BF)
- high organic flux (BF)

pre-OAE 1a

1502

Fig. 8. Paleoceanographic reconstruction of bottom- and surface-water conditions in the Cismon Core from the late Barremian to the early late Aptian. See text for explanations.

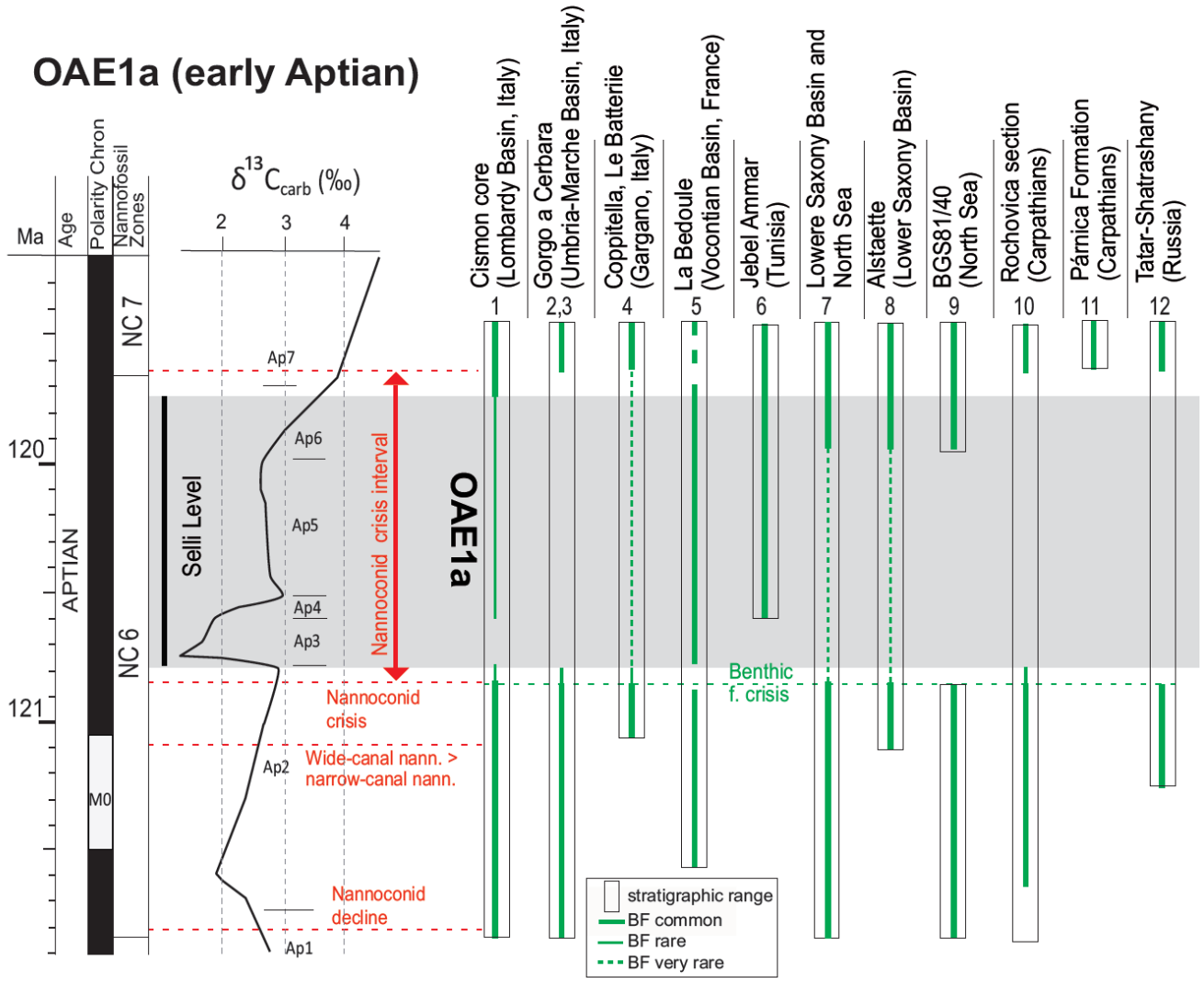

Fig. 9. Synthesis of the benthic foraminiferal abundance data across OAE 1a according to this study and data from the literature, as follows: 1) this study; 2) Coccioni et al., 1992; 3) Patruno et al., 2015; 4) Cobianchi et al., 1999; 5) Moullade et al., 2015; 6) Elkhazri et al., 2013; 7) Mutterlose and Böckel, 1998; 8) von Bargen and Lehmann, 2014; 9) Rückheim et al., 2006; 10) Michalík et al., 2008; 11) Józsa et al., 2016; 12) Zorina et al., 2017.

Tables

BENTHIC FORAMINIFERA	MORPHOGROUPS				OXYGEN			ORGANIC FLUX			REFERENCES
	Epifauna	Shallow Epifauna	Shallow Infauna	Infauna	Low	Middle	High	Low	Middle	High	
Ammodiscus	X	X	X								1, 6, 9, 10, 11, 13, 17, 18
Astacolus	X		X	X							1, 12, 13, 18, 20
Bathysiphon	X										1, 6, 9, 10, 13, 19, 20
Dentalina	X		X								1, 4, 18
Dorothia				X							1, 3, 10, 19, 20
Gavelinella	X										1, 3, 10, 14, 15, 17, 20
Glomospira	X	X	X								1, 2, 3, 9, 10, 13, 17, 19
Gyroidina	X		X								1, 10, 15
Haplophragmoides		X	X	X							2, 3, 6, 13, 15, 17, 18, 19
Hippocrepina	X										6, 7
Laevidentalina			X	X							5, 12, 13, 14, 15, 16, 18, 20
Lenticulina	X		X	X							1, 4, 10, 12, 13, 18, 20
Pleurostomella			X								1, 4, 10, 12, 13, 19
Reophax			X	X							1, 5, 9, 13, 15, 18, 19, 21
Rhizammina	X										1, 2, 3, 5, 6, 8, 9, 11, 13, 15, 17, 23
Verneuilinoides				X							3, 7, 9, 11, 15, 22, 23

Table 1. Paleoecological preferences of benthic foraminifera according to their morphogroups based on previous studies, as follows: Koutsoukos, (1989)[1]; Kuhnt and Kaminski, (1989)[2]; Koutsoukos and Hart, (1990)[3]; Kaiho, (1994)[4]; Tyszka, (1994)[5]; Nagy el al. (1995)[6]; Kuhnt, (1995)[7]; Kaminski and Kuhnt, (1995)[8]; van Den Akker et al. (2000)[9]; Frenzel, (2000)[10]; Szarek et al. (2000)[11]; Holbourn et al. (2001)[12]; Alegret et al. (2003)[13]; Friedrich and Erbacher, (2006)[14]; Rückheim et al. (2006)[15]; Friedrich and Hemleben, (2007)[16]; Cetean et al. (2008)[17]; Reolid et al. (2008)[18]; Cetean et al. (2011)[19]; Koch and Friedrich, (2012)[20]; Reolid and Ruiz, (2012)[21]; Patruno et al. (2015)[22]; Józsa, (2017)[23].

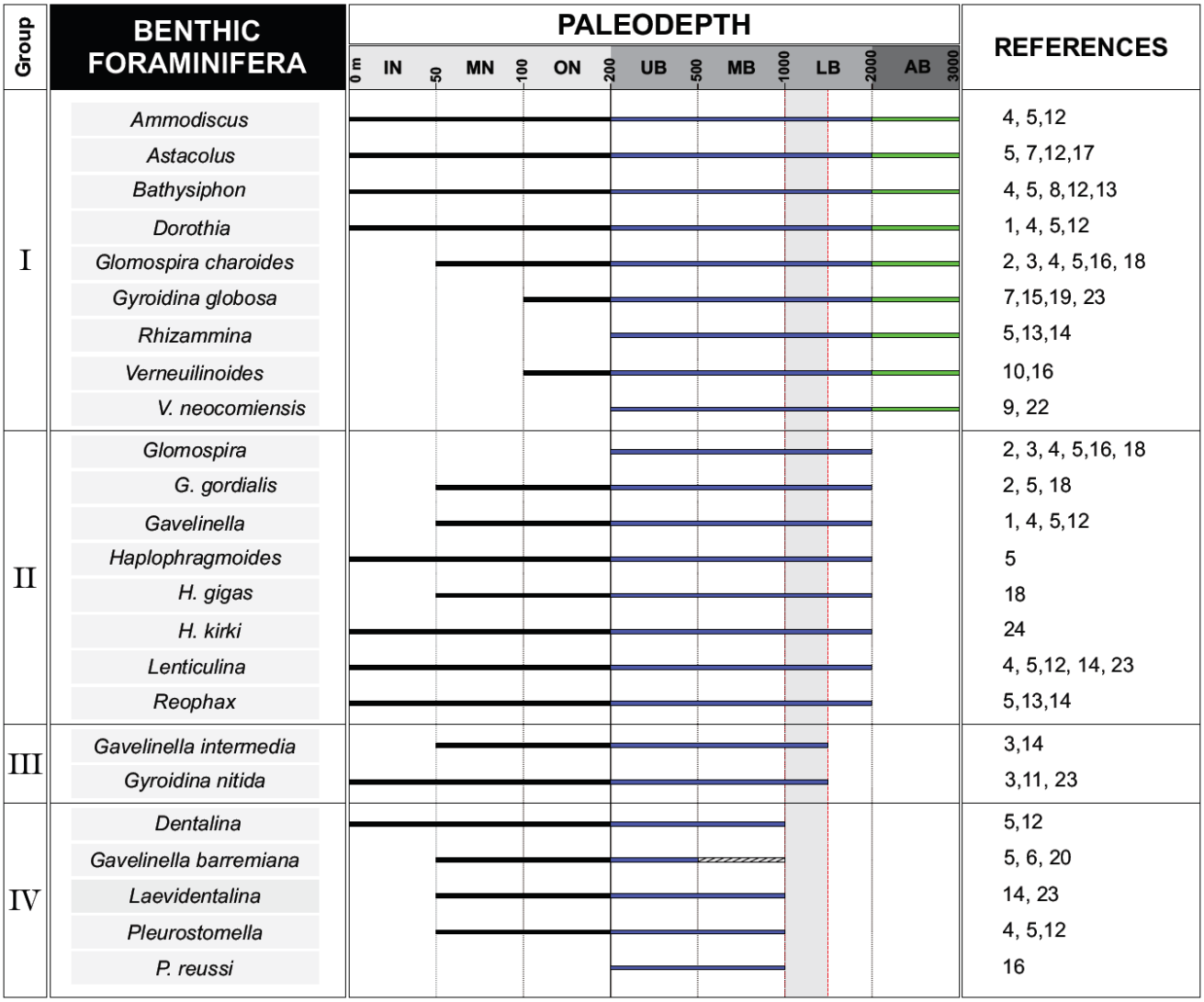

Table 2. Paleobathymetric preferences of benthic foraminiferal taxa identified in the Cismon Core based on different sources, as follows: Sliter and Baker, (1972)[1]; Bock, (1979)[2]; Nygon and Olson, (1984)[3]; De Azevedo et al. (1987)[4]; Koutsoukos, (1989)[5]; Riegraf, (1989)[6]; Saint-Marc, (1992)[7]; Nagy et al. (1995)[8]; Kuhnt, (1995)[9]; Kaminski et al. (1999)[10]; Schnack, (2000)[11]; Frenzel, (2000)[12]; van Den Akker, et al. (2000)[13]; Holbourn et al. (2001)[14]; Alegret et al. (2003)[15]; Szydło, (2004)[16]; Haig, (2005)[17]; Kaminski and Gradstein, (2005)[18]; Moullade et al. (2005)[19]; Tyszka, (2006)[20]; Bindiu et al. (2013)[21]; Holbourn et al. (2013)[22]; Aschckenazi-Polivoda et al. (2018)[23]**.** For this study will be adopted the paleobathymetric subdivision (Nyong and Olsson, 1984 and van Morkhoven et al., 1986): inner-neritic (IN: 0–50 m), middle-neritic (MN: 50–100 m), outer-neritic (ON: 100–200 m), upper bathyal (UB: 200–500 m), middle bathyal (MB: 500–1000 m), lower bathyal (LB: 1000–2000 m) and abyssal

(AB: > 3000 m). The grey band indicates the inferred paleobathymetry for the Cismon Core based on the composition of the benthic foraminiferal assemblages.

Supplementary Data

Comparison between the benthic foraminifera and calcareous plankton records the Cismon Core and the Gorgo a Cerbara section **(see Figure S1)**

Here we provide a comparison of the most important bioevents detected in benthic foraminifera, planktonic foraminifera, and calcareous nannofossils across the OAE 1a at Gorgo a Cerbara and Cismon Core. The two sections show many similarities that can be extrapolated from Supplementary Figure 1 and a few main differences that are commented as follows:

1) The sampling resolution and the methodology adopted for the benthic foraminifera study are different. The benthic foraminiferal sampling resolution applied at Cismon along a 38.05 m thick section (159 samples) is from 5 to 50 cm (from 8 m to 31.29 m) and from 12 to 170 cm in the lower part (31.29 m – 46.75 m). Thus, it is higher compared to the 42 samples along the 33.06 m-thick section at Gorgo a Cerbara.
2) The size-fractions of the washed residues studied for benthic foraminifera are smaller for the Cismon (> 63 μm) compared to the Gorgo Cerbara (> 125 μm). This observation could explain the distribution of the genus *Verneuilinoides*, which is more abundant in the small-sized fraction > 63 μm of the upper Barremian samples of the Cismon Core compared to the equivalent stratigraphic interval at Gorgo a Cerbara.
3) In the Cismon Core, planktonic foraminifera are present within the Selli Level, although in low numbers and few samples are barren, whereas they are completely absent in the Selli Level at Gorgo a Cerbara (Coccioni et al., 1992; Coccioni, 2019). Moreover, at Gorgo a Cerbara, the 26 cm-thick-interval below the Selli level is characterized by a marked decrease in the planktonic foraminiferal abundance and diversity, and the assemblage is composed of only poorly preserved trochospiral hedbergellids (lower critical interval: Coccioni et al., 1992). On the contrary, in the equivalent stratigraphic interval in the Cismon Core, planktonic foraminifera do

not show a significant decrease in abundance, although, similar to Gorgo a Cerbara, the assemblage is dominated by common trochospiral taxa.

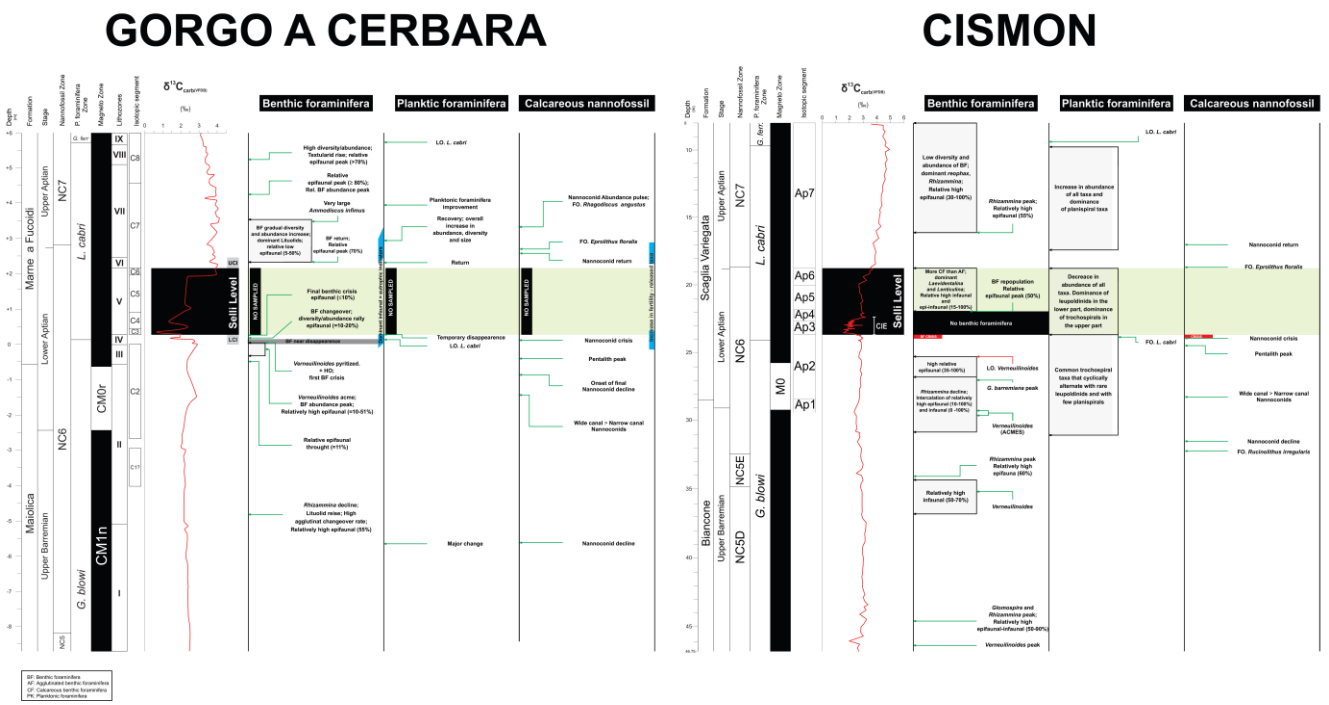

Supplementary data, Figure S1. Comparison of the benthic foraminifera, planktonic foraminifera and calcareous nannofossil assemblage data across the Barremian-Aptian interval from the Gorgo a Cerbara section (Italy) and the Cismon Core (Italy, this study). Data from Gorgo a Cerbara: benthic foraminifera, planktonic foraminifera, and calcareous nannofossil after Coccioni et al. (1992); Patruno et al. (2015) and Coccioni (2019). $\delta^{13}C_{carb}$ data are after Stein et al. (2011) and Li et al. (2016). The carbon isotopic segments Ap1 to Ap7 are after Bottini et al. (2015). Data from Cismon: benthic foraminifera (this work), planktonic foraminifera after Barchetta (2015) and this study, calcareous nannofossil after Erba et al. (1999, 2010). $\delta^{13}C_{carb}$ data after Erba et al. (1999) and Méhay et al. (2009). The carbon isotopic segments C1-C8 are after Menegatti et al. (1998).

Barchetta, A., 2015. The Tethys (Cismon core) and Pacific (DSDP Site 463) Ocean record of OAE1a: a taxonomic and quantitative analysis of planktonic foraminifera and their biological response across the Selli Level equivalent. Doctoral Thesis. Università degli Studi di Milano. Milano, Italy. 228 p. (https://air.unimi.it/handle/2434/260289).

Coccioni, R., Erba, E., Premoli Silva, I., 1992. Barremian-Aptian calcareous plankton biostratigraphy from Gorgo Cerbara section (Marche, central Italy) and implications for plankton evolution. Cretaceous Res. 13, 517-537.

Coccioni, R., 2019. Revised upper Barremian–upper Aptian planktonic foraminiferal biostratigraphy of the Gorgo a Cerbara section (central Italy). Newsl Stratigr. DOI: 10.1127/nos/2019/0539

Erba, E., Channell, J. E. T., Claps, M., Jones, C., Larson, R. L., Opdyke, B., Premoli Silva, I., Riva, A., Salvini, G., Torricelli, S., 1999. Integrated stratigraphy of the Cismon Apticore (Southern Alps, Italy): A "reference section" for the Barremian-Aptian interval at low latitudes. J. Foraminiferal Res. 29, 371-391.

Erba, E., Bottini, C., Weissert, J. H., Keller, C.E., 2010. Calcareous nannoplankton response to surface-water acidification around Oceanic Anoxic Event 1a. Science. 329, 428-432.

Li, J., Hu, X., Zhao, K., Cai, Y., Sun, T., 2016. Paleoceanographic evolution and chronostratigraphy of the Aptian Oceanic Anoxic Event 1a (OAE1a) to oceanic red bed 1 (ORB1) in the Gorgo a Cerbara section (central Italy). Cretaceous Res. 66, 115-128.

Méhay, S., Keller, C. E., Bernasconi, S. M., Weissert, H., Erba, E., Bottini, C., Hochuli, P. A., 2009. A volcanic CO_2 pulse triggered the Cretaceous Oceanic Anoxic Event 1a and a biocalcification crisis. Geology. 37, 819-822.

Menegatti, A. P., Weissert, H., Brown, R. S., Tyson, R. V., Farrimond, P., Strasser, A., Caron, M., 1998. High-resolution $\delta^{13}C$ stratigraphy through the early Aptian "Livello Selli" of the Alpine Tethys. Paleoceanography. 13, 530-545.

Patruno, S., Triantaphyllou, M. V., Erba, E., Dimiza, M. D., Bottini, C., Kaminski, M. A., 2015. The Barremian and Aptian stepwise development of the 'Oceanic Anoxic Event 1a' (OAE 1a) crisis: Integrated benthic and planktic high-resolution palaeoecology along the Gorgo a Cerbara stratotype section (Umbria–Marche Basin, Italy). Palaeogeogr. Palaeoclimatol. Palaeoecol. 424, 147-182.

Stein, M., Föllmi, K.B., Westermann, S., Godet, A., Adatte, T., Matera, V., Fleitmann, D., Berner, Z., 2011. Progressive palaeoenvironmental change during the late Barremian–early Aptian as prelude to Oceanic Anoxic Event 1a: Evidence from the Gorgo a Cerbara section (Umbria-Marche basin, central Italy). Palaeogeogr. Palaeoclimatol. Palaeoecol. 302, 396-406.

Supplementary data, Table S1. Distribution chart of benthic foraminifera at Cismon Core (xls.).